

Structure–Activity Relationships for Amide-, Carbamate-, And Urea-Linked Analogues of the Tuberculosis Drug (6S)-2-Nitro-6-[[4-(trifluoromethoxy)benzyl]oxy]-6,7-dihydro-5H-imidazo[2,1-*b*][1,3]oxazine (PA-824)

Adrian Blaser,[†] Brian D. Palmer,[†] Hamish S. Sutherland,[†] Iveta Kmentova,[†] Scott G. Franzblau,[‡] Baojie Wan,[‡] Yuehong Wang,[‡] Zhenkun Ma,[§] Andrew M. Thompson,^{*,†} and William A. Denny[†]

[†]Auckland Cancer Society Research Centre, School of Medical Sciences, The University of Auckland, Private Bag 92019, Auckland 1142, New Zealand

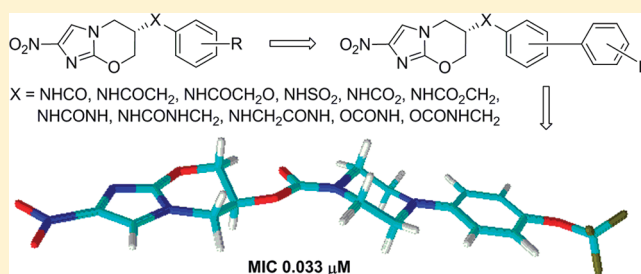
[‡]Institute for Tuberculosis Research, College of Pharmacy, University of Illinois at Chicago, 833 South Wood Street, Chicago, Illinois 60612, United States

[§]Global Alliance for TB Drug Development, 40 Wall Street, New York 10005, United States

S Supporting Information

ABSTRACT: Analogues of clinical tuberculosis drug (6S)-2-nitro-6-[[4-(trifluoromethoxy)benzyl]oxy]-6,7-dihydro-5H-imidazo[2,1-*b*][1,3]oxazine (PA-824), in which the OCH₂ linkage was replaced with amide, carbamate, and urea functionality, were investigated as an alternative approach to address oxidative metabolism, reduce lipophilicity, and improve aqueous solubility. Several soluble monoaryl examples displayed moderately improved (~2- to 4-fold) potencies against replicating *Mycobacterium tuberculosis* but were generally inferior inhibitors under anaerobic (nonreplicating) conditions.

More lipophilic biaryl derivatives mostly displayed similar or reduced potencies to these in contrast to the parent biaryl series. The leading biaryl carbamate demonstrated exceptional metabolic stability and a 5-fold better efficacy than the parent drug in a mouse model of acute *M. tuberculosis* infection but was poorly soluble. Bioisosteric replacement of this biaryl moiety by arylpiperazine resulted in a soluble, orally bioavailable carbamate analogue providing identical activity in the acute model, comparable efficacy to OPC-67683 in a chronic infection model, favorable pharmacokinetic profiles across several species, and enhanced safety.



INTRODUCTION

With levels of tuberculosis (TB) incidence at their highest ever, there is an urgent need for new drugs with greater efficacy, safety, and affordability that can reduce the high pill burden and shorten lengthy treatment times (a minimum of 6 months for drug-susceptible TB with current therapy).^{1,2} This is particularly true in cases of multi- and extensively drug resistant tuberculosis (MDR-TB and XDR-TB), and in persistent forms of the disease, where the existing drugs are less effective.³ After more than four decades of minimal effort in this regard, intense recent efforts spearheaded by the Global Alliance for Tuberculosis Drug Development (TB Alliance, founded February 2000) have led to more than 10 agents in current clinical trials.^{4,5} The bicyclic nitroimidazole analogues, PA-824 (1)⁶ and OPC-67683 (2),⁷ currently in phase II clinical trials, are of particular interest because these drugs are active against both replicating and nonreplicating persistent *Mycobacterium tuberculosis* (*M. tb*) infections in animal models and are useful against MDR-TB.^{4,5} Compound 1 reportedly acts via a bioreductive mechanism to cause both cell wall inhibition and

respiratory poisoning (via nitric oxide release) under aerobic and anaerobic conditions, respectively.^{6,8,9} Recent clinical data for 1, indicating excellent early bactericidal activity at 200 mg/day,¹⁰ has been shown to correlate well with the time-dependent activity observed in vivo, where percentage time that the free drug concentration exceeds the minimum inhibitory concentration (MIC) was found to be the crucial parameter for dose optimization.¹¹

In considering the challenges for further antituberculosis drug development,¹ it is useful to reiterate here some key desirable attributes for a new drug in terms of pharmacological profile and safety. These include good stability under various conditions, high oral bioavailability, sufficient lung penetration, a lengthy elimination half-life (suitable for once-daily or less frequent dosing), acceptable protein binding, freedom from genotoxicity/mutagenicity, satisfactory cardiac safety (minimal hERG inhibition), and avoidance of other toxicities.⁴ An absence

Received: September 14, 2011

Published: December 8, 2011

of drug–drug interactions is particularly critical with combination treatments but also because HIV coinfection is a significant problem (estimated at up to 15% of the global TB burden; ~2 million people), especially in Africa.^{2,12} The first-line TB drug rifampicin, for example, is a potent inducer of cytochrome P450 (CYP) enzymes (especially CYP3A4) that can metabolize comedications such as antiretroviral agents (mostly HIV protease inhibitors), leading to subtherapeutic concentrations; another first-line TB drug, isoniazid, is a CYP inhibitor, which can cause toxicities due to higher than expected levels of co-administered drugs.^{1,4} Beyond these properties, the new agent should further display good bactericidal activity and good sterilizing activity (against persistent bacilli), with no cross-resistance to current drugs, and must be affordable.⁴ These are characteristics that we have been pursuing for second-generation analogues of **1**. Finally, regarding challenges encountered in early stage drug development, the ability of *M. tb* to exist in a range of metabolic states (such that subpopulations of bacteria in different microenvironments in vivo are able to exhibit differential drug susceptibilities) clearly adds additional complexity both to the discovery of structure–activity relationships (SARs) and to the possible correlation of in vitro potency with in vivo efficacy.^{3,4,12}

Following on from our initial investigations^{13–15} of (hetero)-biaryl side chain analogues of **1** (including early biphenyl lead **3**) that culminated in the more soluble, orally bioavailable pyridine derivative **4** (having markedly superior efficacies to **1** in mouse models of both acute and chronic *M. tb* infection), we recently described¹⁶ an SAR study of alternative side chain ether linkages (to OCH₂), seeking new candidates with both high efficacy and enhanced metabolic stability (reduced toxicity potential) (Figure 1). The latter issue was related to the possible muta-

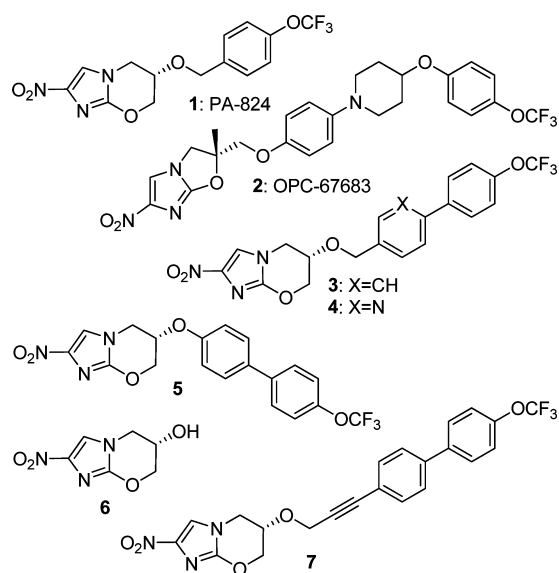


Figure 1. Structures of antitubercular agents.

genicity of smaller metabolites formed by oxidative cleavage of the benzyl ether (or picolyl ether) side chain based upon reported Ames data for 6-nitroimidazooxazoles.¹⁷ While compounds such as **1** and **2** are not mutagenic (both in vitro and in vivo),^{6,7} and **1** has displayed excellent safety in clinical trials,¹⁸ we deemed that removal of, or substitution on, the benzylic methylene moiety should be evaluated as first options to enhance compound stability and further minimize any possible

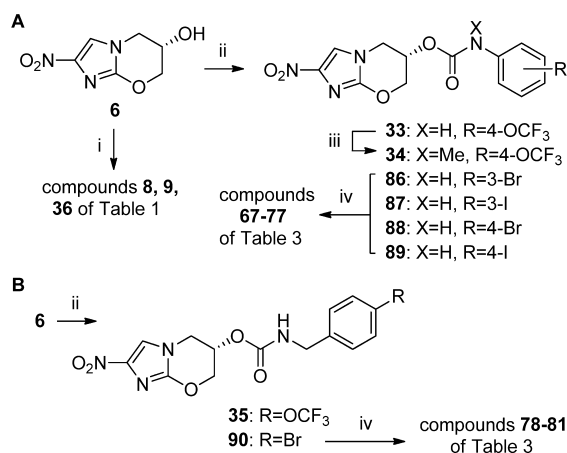
toxicity risks associated with molecular fragmentation. However, α -methyl substitution, described¹⁹ as a possible means to suppress oxidative metabolism of benzyl ethers, proved an ineffective stabilization strategy in our hands. In contrast, removal of the benzylic methylene provided one biaryl analogue (**5**) that exhibited reasonable efficacy in the acute model (8-fold better than **1**) and negligible fragmentation to alcohol metabolite **6** in liver microsomes. Unfortunately, both this compound (**5**) and the other leading candidate that arose from this ether modification study (**7**: 89-fold better than **1** in the same in vivo model) were poorly soluble (<0.5 $\mu\text{g/mL}$ in water at pH = 7) and pyridine analogues of these were less effective. Therefore, additional linker options were considered to better enable us to address this metabolic stability issue.

More than a decade ago, Baker et al. (PathoGenesis Corporation) disclosed the high in vitro potencies of a few amide, urea, and carbamate-linked analogues of **1** against *Mycobacterium bovis* (similar data against *M. tb* were not provided).²⁰ Very recently, more soluble amine-linked congeners of **1** were also examined²¹ (by Novartis), but no reports have further investigated the former linker classes. In this current paper, we therefore describe replacement of the OCH₂ linkage of **1** (and its isomers, selected biaryl analogues, and their bioisosteres) with various amide, carbamate, and urea functionality and evaluate this as a possible alternative strategy to circumvent oxidative metabolism, reduce compound lipophilicity, and improve aqueous solubility (while maintaining reasonable in vivo efficacy) in order to provide a superior TB drug candidate with enhanced safety.

CHEMISTRY

The reference benzyl ethers **8**²² and **9**, together with acetamide **36**²² (previously reported by amide formation on an acid precursor), were prepared by NaH-assisted alkylation of the known²⁰ oxazine alcohol **6** and the requisite halides (Scheme 1).

Scheme 1^a

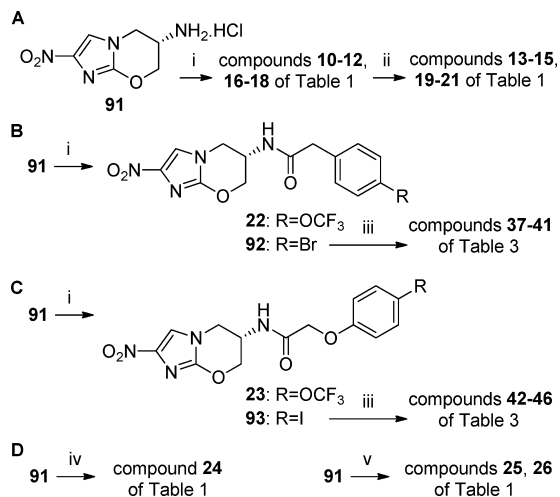


^aReagents and conditions: (i) 2-/3-O-CF₃BnBr or 4-O-CF₃PhNHCOCH₂Cl, NaH, DMF, 0–20 °C, 2.5–6 h; (ii) RPhNCO or RBnNCO, CuCl, DMF, 20 °C, 2–4 h; (iii) MeI, NaH, DMF, 20 °C, 3 h; (iv) ArB(OH)₂ (or pinacol ester), toluene, EtOH, 2 M K₂CO₃, Pd(dppf)Cl₂ under N₂, reflux, 1–3 h.

The known²⁰ 6-*O*-carbamates **33** and **35**, as well as halide analogues **86**–**90** (needed for the synthesis of biaryl derivatives **67**–**81** using Suzuki coupling), were also derived from **6** via Cu(I)-catalyzed condensation with aryl isocyanates; *N*-methylation

of **33** then yielded **34**. The required 4-(trifluoromethoxy)benzyl isocyanate²³ was made by Curtius rearrangement of the acyl azide (as reported).

Synthesis of the remaining linker variants began with the known^{20,21} chiral amine **91** (stored as its hydrochloride salt for improved stability). Acylation or sulfonylation reactions of **91** using the relevant acyl or sulfonyl chlorides (sourced from the available acids via standard procedures where necessary) yielded the desired amides (**10–12**, **22**, **23**, **92**, and **93**) and sulfonamides (**16–18**), which were subsequently *N*-methylated in a few cases (Scheme 2A–C). Halides **92** and **93** were also

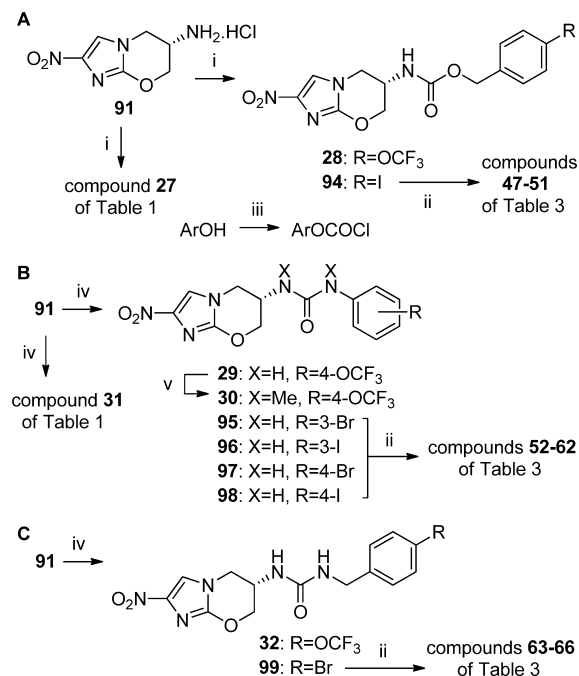
Scheme 2^a

^aReagents and conditions: (i) ArCOCl or ArSO₂Cl or RPhOCH₂COCl, DIPEA, DMF, or THF or dioxane, 20 °C, 1–4 h; (ii) MeI, NaH or K₂CO₃, DMF, 0 or 20 °C, 1.5–3 h; (iii) ArB(OH)₂, toluene, EtOH, 2 M K₂CO₃, Pd(dppf)Cl₂ under N₂, reflux, 1–3 h; (iv) 4-OCF₃PhCHO, NaBH₃CN, AcOH, DMF, 20 °C, 2.5 h; (v) 4-OCF₃PhCOCH₂Br or 4-OCF₃PhNHC(=O)CH₂Cl, DIPEA, DMF, 20–65 °C, 2.5–4.5 h.

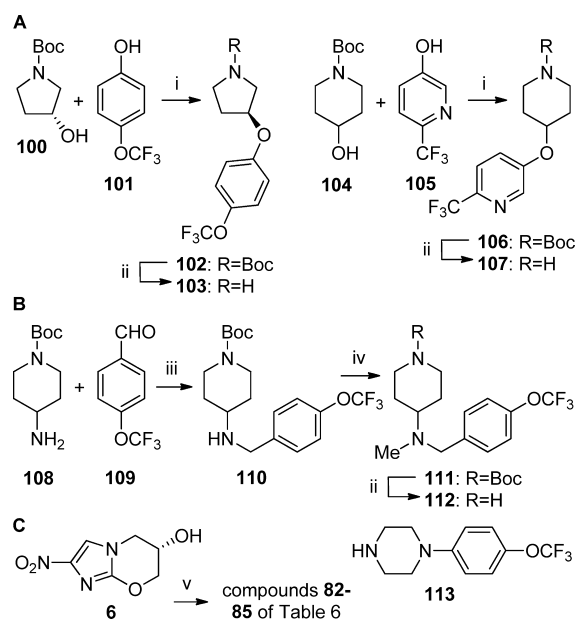
elaborated to biaryl derivatives **37–46** by Suzuki coupling. The 6-amino congener of **1** (**24**)²¹ was prepared via reductive alkylation of **91** (as reported), whereas extended linker analogues (**25** and **26**) were made in poor yields from unoptimized reactions employing the commercial halides (Scheme 2D).

Aryl chloroformates, required for the assembly of *N*-carbamates **27**, **28**,²⁰ and **94**, were generated by base-catalyzed reaction of triphosgene with the appropriately substituted phenol or benzyl alcohol^{24,25} and reacted in situ with **91** (Scheme 3A). Alternatively, treatment of **91** with aryl isocyanates (using NMM and catalytic dibutyltin diacetate) gave ureas **29** and **32** and their halide analogues **95–99**; use of the related aryl isothiocyanate also led to thiourea **31** (Scheme 3B,C). *N*-Methylation on both nitrogen atoms of urea **29** provided **30**, while Suzuki couplings on halides **94–99** produced compounds **47–66**.

Finally, the *O*-carbamates **82–85** were formed by chloroformylation of alcohol **6**, followed by one-pot coupling with the cyclic amine derivatives **103**, **107**, **112**, or **113** (Scheme 4). The required intermediates **103** and **107** were prepared via Mitsunobu reactions on the *N*-Boc hydroxy-amines **100** and **104**, followed by Boc deprotection. Synthesis of **112** was achieved via successive Schiff base formation between amine

Scheme 3^a

^aReagents and conditions: (i) ArOCOC(=O)Cl, DIPEA, CH₂Cl₂, 20 °C, 1.5–3 h; (ii) ArB(OH)₂ (or pinacol ester), toluene, EtOH, 2 M K₂CO₃, Pd(dppf)Cl₂ under N₂, reflux, 1–3 h; (iii) CO(OC(=O)Cl)₂, DIPEA, CH₂Cl₂, 0–20 °C, 2–4 h; (iv) ArNCO or 4-OCF₃PhNCS, NMM, Bu₂Sn(OAc)₂, DMF, 20 °C, 2–5 h; (v) MeI, NaH, DMF, 0–20 °C, 1 h.

Scheme 4^a

^aReagents and conditions: (i) DEAD, PPh₃, THF, reflux, 5 h; (ii) TFA, CH₂Cl₂, 20 °C, 1–4 h; (iii) MeOH, reflux, 4 h, then NaBH₄, 20 °C, 30 min; (iv) MeI, K₂CO₃, Me₂CO, 20 °C, 18 h; (v) CO(OC(=O)Cl)₂, Et₃N, THF, 5–20 °C, 2 h, then **103**, **107**, **112**, or **113**, THF, 20 °C, 2 h.

108 and aldehyde **109**, in situ reduction with NaBH₄ (to give **110**), *N*-methylation (**111**) and deprotection, while **113**²⁶ was obtained using Buchwald coupling on *N*-Boc piperazine.

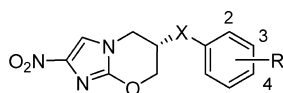
RESULTS AND DISCUSSION

A total of 68 new and 10 known analogues of **1** in which the OCH₂ linkage was modified or replaced with amine, amide, carbamate, and urea functionality were initially screened in two in vitro assays for determination of their aerobic and anaerobic activities (minimum inhibitory concentrations, MICs) against *M. tb* strain H37Rv (Tables 1, 3 and 6). The MABA (aerobic) assay²⁷ assessed growth inhibition of replicating *M. tb* over an 8-day exposure, with the MIC being the lowest drug concentration to effect an inhibition of >90% (recorded values being the mean of 2–5 independent determinations ± SD). The luminescence-based low-oxygen-recovery (LORA, anaerobic) assay²⁸ further examined compound effects against bacteria in the nonreplicating state that models clinical persistence, using an 11-day exposure to *M. tb* that had first been adapted to low oxygen conditions by extended culture. Screening for antitubercular activity under oxygen depletion conditions (or related stresses) has been recommended as a reasonable starting point for the identification of agents that are better at removing persistent bacteria in vivo to potentially shorten

treatment times.^{4,29} Because **1** displays an alternative mechanism of action under these conditions,^{8,9} it is unsurprising that different SAR trends can result from testing analogues of **1** in these two assays.^{13–16,21} Mammalian cytotoxicity was also evaluated³⁰ against VERO cells (CCL-81, American Type Culture Collection) in a 72 h exposure, using a tetrazolium dye assay. Here, the compounds generally showed very low toxicity, with IC₅₀ values of >128 μM (the highest concentration tested; data not shown) for all except five analogues, none of which showed notable activities.

In addition to these biological assays, the lipophilicities of the new analogues were studied using CLogP estimations obtained from the latest ACD LogP/LogD software (version 12.0; Advanced Chemistry Development Inc., Toronto, Canada); in most cases the compounds in this study were significantly more hydrophilic than their OCH₂-linked counterparts (by up to 1.8 log units). Aqueous solubility data (at pH = 7) were also measured for almost all of the 4-OCF₃ substituted examples; about half of the monoaryl analogues (particularly those containing amine, amide, or urea functionality, Table 1) demonstrated superior results in comparison to **1** itself. For biaryl

Table 1. Physicochemical Properties and MIC Values for Amide, Urea, and Carbamate-Linked Analogues of **1** (Monoaryls)



compd	X	R	CLogP ^a	solubility ^b	MIC ^c (μM)	
					MABA	LORA
8 ^d	OCH ₂	2-OCF ₃	3.49		1.8 ± 0	8.6 ± 1.7
9	OCH ₂	3-OCF ₃	3.29		0.36 ± 0.06	2.1 ± 0.3
1 ^e	OCH ₂	4-OCF ₃	3.11	19	0.50 ± 0.30	2.6 ± 1.4
10	NHCO	2-OCF ₃	2.99		27 ± 7	>64
11	NHCO	3-OCF ₃	2.65		4.9 ± 1.2	>64
12 ^e	NHCO	4-OCF ₃	2.48	109	1.8 ± 0.1	19 ± 2
13	N(Me)CO	2-OCF ₃	2.26		45 ± 18	>64
14	N(Me)CO	3-OCF ₃	2.41		24 ± 8	>64
15	N(Me)CO	4-OCF ₃	1.98	17	22 ± 4	>64
16	NHSO ₂	2-OCF ₃	1.95		>64	>64
17	NHSO ₂	3-OCF ₃	2.24		>64	>64
18	NHSO ₂	4-OCF ₃	1.71	6.1	9.7 ± 2.2	>64
19	N(Me)SO ₂	2-OCF ₃	3.05		20 ± 6	45 ± 4
20	N(Me)SO ₂	3-OCF ₃	3.40		12 ± 4	64 ± 6
21	N(Me)SO ₂	4-OCF ₃	2.98	15	0.53 ± 0.04	22 ± 1
22 ^e	NHCOCH ₂	4-OCF ₃	2.56	64	0.27 ± 0.03	21 ± 6
23 ^f	NHCOCH ₂ O	4-OCF ₃	2.40	43	0.16 ± 0.05	10 ± 4
24 ^f	NHCH ₂	4-OCF ₃	2.95	131	0.22 ± 0.02	5.3 ± 1.3
25	NHCH ₂ CO	4-OCF ₃	1.97	21	7.6 ± 0.6	>64
26	NHCH ₂ CONH	4-OCF ₃	2.54		0.70 ± 0.22	46 ± 16
27	NHCO ₂	4-OCF ₃	2.58		>64 ^g	>64 ^g
28 ^e	NHCO ₂ CH ₂	4-OCF ₃	2.86		0.15 ± 0.04	11 ± 3
29 ^e	NHCONH	4-OCF ₃	2.48	93	0.23 ± 0.01	4.2 ± 0.3
30	NMeCONMe	4-OCF ₃	1.96	38	12 ± 2	>64
31	NHCSNH	4-OCF ₃	2.17	12	8.0 ± 0.2	>64
32	NHCONHCH ₂	4-OCF ₃	2.03	32	0.27 ± 0.07	4.1 ± 0.4
33 ^e	OCNH	4-OCF ₃	2.62	5.4	0.12 ± 0.01	2.7 ± 0.8
34	OCN(Me)	4-OCF ₃	1.75	18	0.21 ± 0.03	5.4 ± 0.8
35 ^e	OCNHCH ₂	4-OCF ₃	2.38	10	0.25 ± 0.02	17 ± 4
36 ^d	OCH ₂ CONH	4-OCF ₃	2.67	68	0.24 ± 0	7.8 ± 0.9

^aCLogP values, calculated using the ACD LogP/LogD prediction software (version 12.0, Advanced Chemistry Development Inc., Toronto, Canada). ^bSolubility (μg/mL) in water at pH = 7 and 20 °C, determined by HPLC (see Experimental Section). ^cMinimum inhibitory concentration, determined under aerobic (MABA)³⁰ or anaerobic (LORA)²⁸ conditions. Each value is the mean of at least two independent determinations ± SD. ^dRef 22. ^eRef 20. ^fRef 21. ^gUnstable under assay conditions.

compounds (Table 3), replacement of the terminal phenyl ring by pyridine and *meta* linkage of the biaryl moiety gave improved solubility values, as found previously.^{15,16}

An initial examination of direct (monoaryl) analogues of **1** (Table 1) began with a small study investigating the effect of varying the position of the trifluoromethoxy substituent for some relatively rigid amide and sulfonamide linkers (NHCO, NMeCO, NHSO₂, NMeSO₂; note that we elected to consider only this particular substituent based on previous studies^{13–16} indicating broad utility and superior *in vivo* efficacy). In the parent OCH₂-linked series, the 2-OCF₃ analogue **8** was the least effective in both replicating and nonreplicating *M. tb* assays, compared with the 3- and 4-OCF₃ analogues **9** and **1**. This pattern also held for the amide and sulfonamide linkers (**10–21**), where 4-OCF₃ was preferred; therefore, the latter positioning was retained for all of the remaining linker analogues, enabling a direct comparison with **1**. However, compounds **10–21** were generally much less active than their corresponding OCH₂-linked congeners, likely due to the increased rigidity imposed, which could project the phenyl ring at an inappropriate orientation in the binding site of the activating enzyme. A similar reduction in potency was recently observed for a phenyl ether variant of **1** (X = O),¹⁶ while previous studies^{13,15} have also shown consistent and significant differences in the mean MIC potencies of *ortho*-, *meta*-, and *para*-linked biaryl analogues, consistent with an elongated but constricted side chain binding site. *N*-Methylation was disfavored in the amide series (**13–15**) but was unexpectedly activating in the less impressive sulfonamide series, with the 4-OCF₃ analogue **21** showing equivalent aerobic potency to the similarly lipophilic **1** (but 8.5-fold lower potency under anaerobic assay conditions). Homologation of the more soluble amide **12** (to the less constrained **22**) significantly improved the MABA MIC value (~7-fold; 0.27 μM) although the anaerobic activity remained weak (21 μM). Further known linker extension (**23**)²¹ provided a more modest (~2-fold) additional potency gain in both MIC assays and still permitted good aqueous solubility (43 μg/mL). Analogous improvements in aerobic MIC potency with longer flexible linkers have been noted in earlier reports.^{16,21}

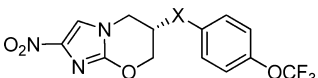
The previously described 6-amino analogue of **1** (**24**)²¹ provided greater solubility than **1** and had better activity against replicating *M. tb* (~2-fold), as reported. However, this compound seemed slightly less effective than **1** under nonreplicating conditions, and ketone- or amide-containing extended linker derivatives of this (**25**, **26**), designed to introduce some conformational restriction, were much worse. Alternatively, the novel *N*-carbamate **27**, while quite stable in nonpolar solvents, was surprisingly not sufficiently stable in DMSO (the solvent employed to dissolve test compounds for these *in vitro* assays), resulting in very poor MIC results. In marked contrast to this, the known²⁰ homologue of **27** (**28**), an isomer of the more hydrophilic extended amide **23** above, gave very good MABA data (0.15 μM), being equipotent to **23** in both assays. Furthermore, both the urea analogue of **27** (**29**) and its homologue (**32**) demonstrated a comparable MIC profile to amine **24**, but *N*-methylation (**30**) or thiation (**31**) significantly diminished potency. Encouragingly, urea **29** also showed a 5-fold higher aqueous solubility than **1** (93 μg/mL).

Noting that all of the 6-*N*-linked compounds above had anaerobic activities that were inferior to the 6-OCH₂-linked trial drug **1**, we finally examined a few 6-*O*-linked congeners of the compounds above. Pleasingly, *O*-carbamate **33** displayed an

identical potency to **1** in the LORA assay and was 4-fold more effective in the MABA assay, albeit this compound had inferior aqueous solubility. Unexpectedly, *N*-methylation of **33** (**34**) lowered the CLogP value and improved solubility compared to **33** (~3-fold), although the activity of **34** was concomitantly reduced (~2-fold in both assays). Finally, both homologation of **33** (**35**) and extension of the 6-OCH₂ linker with an amide moiety (**36**) gave inferior results to **33** (notably under nonreplicating conditions), although the latter compound did provide enhanced solubility.

The activities of a few of the compounds in Table 1 against *M. bovis* have been reported previously.²⁰ Against *M. tb*, these compounds were found to be on average about 3-fold less potent but showed a similar rank order of aerobic activity (Table 2). Overall then, the results suggested several possible

Table 2. Comparative Activity of Selected Compounds of Table 1 against *M. bovis* and *M. tb*



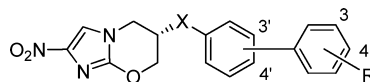
compd	X	MIC (μM)	
		<i>M. bovis</i> ^a	<i>M. tb</i> ^b
1	OCH ₂	0.167	0.50
12	NHCO	1.34	1.8
28	NHCO ₂ CH ₂	0.037	0.15
29	NHCONH	0.039	0.23
33	OCNH	0.039	0.12
35	OCONHCH ₂	0.075	0.25

^aRef 20. ^bThis work.

alternatives to OCH₂ as linking groups for additional analogues of **1**. The seven best of these (NHCOCH₂, NHCOCH₂O, NHCO₂CH₂, NHCONH, NHCONHCH₂, OCONH, and OCONHCH₂) were therefore selected for the syntheses of small series of related compounds bearing predominantly *para*-linked biaryl side chains (Table 3). We have shown previously^{13,15} that for compounds containing the OCH₂ linker, *para*-linked biaryl analogues were substantially more effective than **1** against both replicating and nonreplicating *M. tb*, with *meta*-linked congeners generally providing slightly inferior results but *ortho*-linked compounds being poor, consistent with a long, linear binding site. However, in the current study, we elected to investigate both *para*- and *meta*-linkage for two cases (X = NHCONH, OCONH) where there was greater conformational restriction to allow for the possibility that a *meta*-linked geometry might be more favorable in such instances. On the basis of our earlier findings in the *para*-linked biphenyl series,¹³ showing a significant correlation of aerobic *M. tb* activity with both overall lipophilicity, and with the electron-withdrawing ability of substituents, we selected three such substituents (CF₃, F, OCF₃) for the terminal phenyl ring in addition to pyridine comparators (e.g., 3-aza-4-CF₃) that might enhance aqueous solubility.^{15,16}

To provide a broader assessment of the utility of the selected linkers in this new context, Table 4 compares the activities of the different subseries of biaryl compounds of Table 3 with their corresponding OCH₂-linked analogues by examining the mean MIC values for each subseries having the four common aryl substituents indicated above. This analysis suggests that, for the 4-linked biaryls, all of the new linkers resulted in considerably

Table 3. Physicochemical Properties and MIC Values for Amide, Urea, and Carbamate-Linked Analogues of 1 (Biaryls)



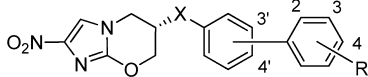
compd	X	link	R	CLogP ^a	solubility ^b	MIC ^c (μM)	
						MABA	LORA
3 ^d	OCH ₂	4'	4-OCF ₃	4.95	1.2	0.035 \pm 0.015	1.3 \pm 0.1
37	NHCOCH ₂	4'	4-CF ₃	3.45		0.44 \pm 0.15	23 \pm 4
38	NHCOCH ₂	4'	4-F	3.48		0.33 \pm 0.11	11 \pm 2
39	NHCOCH ₂	4'	4-OCF ₃	4.40	1.8	0.22 \pm 0.03	5.0 \pm 0.1
40	NHCOCH ₂	4'	3-aza, 4-CF ₃	1.69		0.46 \pm 0.01	>32
41	NHCOCH ₂	4'	3-aza, 4-F	2.31		0.68 \pm 0.28	>32
42	NHCOCH ₂ O	4'	4-CF ₃	3.12		0.25 \pm 0.01	>32
43	NHCOCH ₂ O	4'	4-F	3.14		0.17 \pm 0.05	26 \pm 1
44	NHCOCH ₂ O	4'	4-OCF ₃	4.07	0.96	0.18 \pm 0.07	25 \pm 4
45	NHCOCH ₂ O	4'	3-aza, 4-CF ₃	1.35		0.69 \pm 0.15	30 \pm 2
46	NHCOCH ₂ O	4'	3-aza, 4-F	1.97		0.69 \pm 0.25	31 \pm 1
47	NHCO ₂ CH ₂	4'	4-CF ₃	3.75		0.08 \pm 0.02	4.5 \pm 2.0
48	NHCO ₂ CH ₂	4'	4-F	3.78		0.085 \pm 0.025	4.2 \pm 0.9
49	NHCO ₂ CH ₂	4'	4-OCF ₃	4.70	0.67	0.11 \pm 0.01	5.0 \pm 2.1
50	NHCO ₂ CH ₂	4'	3-aza, 4-CF ₃	1.99		0.23 \pm 0.01	4.7 \pm 1.3
51	NHCO ₂ CH ₂	4'	3-aza, 4-F	2.61		0.34 \pm 0.10	4.3 \pm 0.6
52	NHCONH	3'	4-CF ₃	2.18		0.035 \pm 0.005	3.6 \pm 0.6
53	NHCONH	3'	4-F	2.20		0.03 \pm 0	3.8 \pm 1.2
54	NHCONH	3'	4-OCF ₃	3.13	3.0	0.25 \pm 0.10	5.8 \pm 3.4
55	NHCONH	3'	3-aza, 4-CF ₃	0.42		0.22 \pm 0.01	13 \pm 1
56	NHCONH	3'	3-aza, 4-F	1.03		0.23 \pm 0.01	15 \pm 1
57	NHCONH	4'	4-CF ₃	3.45		0.19 \pm 0.03	>32
58	NHCONH	4'	4-F	3.48		1.3 \pm 0.5	9.1 \pm 3.4
59	NHCONH	4'	4-OCF ₃	4.40	0.17	0.06 \pm 0	18 \pm 5
60	NHCONH	4'	3-aza, 4-CF ₃	1.69		0.17 \pm 0.07	17 \pm 3
61	NHCONH	4'	3-aza, 4-F	2.31		0.24 \pm 0.01	11 \pm 2
62	NHCONH	4'	4-aza, 3-CF ₃	2.21		0.36 \pm 0.14	13 \pm 0
63	NHCONHCH ₂	4'	4-CF ₃	2.92		0.32 \pm 0.13	>32
64	NHCONHCH ₂	4'	4-F	2.94		0.11 \pm 0.02	26 \pm 3
65	NHCONHCH ₂	4'	4-OCF ₃	3.87	0.94	1.0 \pm 0.2	32 \pm 16
66	NHCONHCH ₂	4'	3-aza, 4-CF ₃	1.16		0.40 \pm 0.21	>32
67	OCONH	3'	4-CF ₃	3.26		0.04 \pm 0.0	1.0 \pm 0.4
68	OCONH	3'	4-F	3.28		0.027 \pm 0.005	1.5 \pm 0.4
69	OCONH	3'	4-OCF ₃	4.21	0.07	0.06 \pm 0	0.85 \pm 0.25
70	OCONH	3'	3-aza, 4-CF ₃	1.50	5.8	0.11 \pm 0.01	2.9 \pm 0.8
71	OCONH	3'	3-aza, 4-F	2.11		0.24 \pm 0.01	5.8 \pm 2.0
72	OCONH	4'	4-CF ₃	3.92		0.055 \pm 0.005	>32
73	OCONH	4'	4-F	3.94		1.3 \pm 0.4	18 \pm 4
74	OCONH	4'	4-OCF ₃	4.86	0.06	0.05 \pm 0.01	>32
75	OCONH	4'	3-aza, 4-CF ₃	2.15		0.25 \pm 0	4.1 \pm 0.4
76	OCONH	4'	3-aza, 4-F	2.77		0.13 \pm 0.04	4.3 \pm 1.7
77	OCONH	4'	4-aza, 3-CF ₃	2.67		0.75 \pm 0.11	6.2 \pm 2.7
78	OCONHCH ₂	4'	4-CF ₃	3.27		0.24 \pm 0.01	>32
79	OCONHCH ₂	4'	4-F	3.30		0.11 \pm 0.01	4.5 \pm 0.8
80	OCONHCH ₂	4'	4-OCF ₃	4.22	0.34	0.52 \pm 0.08	2.4 \pm 0.8
81	OCONHCH ₂	4'	3-aza, 4-CF ₃	1.51		0.69 \pm 0.19	11 \pm 6

^aCLogP values, calculated using the ACD LogP/LogD prediction software (version 12.0, Advanced Chemistry Development Inc., Toronto, Canada). ^bSolubility ($\mu\text{g}/\text{mL}$) in water at pH = 7 and 20 °C, determined by HPLC (see Experimental Section). ^cMinimum inhibitory concentration, determined under aerobic (MABA)³⁰ or anaerobic (LORA)²⁸ conditions. Each value is the mean of at least two independent determinations \pm SD. ^dRef 13.

lower activity than the parent OCH₂ linker in both the aerobic and anaerobic assays (X/OCH₂ ratios mostly >10), with only the *N*-linked carbamate analogues (47–50; the most lipophilic of the 6-acylamino derivatives) showing reasonable overall potencies. In contrast, in the two less lipophilic 3-linked biaryl

subseries investigated, the alternative linkers (X = NHCONH and OCONH) were slightly more effective than OCH₂ in providing activity against replicating *M. tb* (mean MABA MIC values 1.5- to 3.2-fold better) and gave comparable (X = NHCONH) or improved potencies (X = OCONH) in the LORA assay

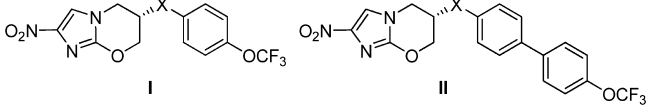
Table 4. Influence of the Linker X on the Mean Inhibitory Potencies of Biaryl Analogues



comps	link	X	ΔCLogP^a	mean MICs (μM)		ratio ^b (X/OCH ₂)	
				MABA	LORA	MABA	LORA
37–40	4'	NHCOCH ₂	−0.55	0.36	>18	13	11
42–45	4'	NHCOCH ₂ O	−0.89	0.32	>28	11	18
47–50	4'	NHCO ₂ CH ₂	−0.25	0.13	4.6	4.6	2.9
52–55	3'	NHCONH	−1.83	0.13	6.6	0.68	1.5
57–60	4'	NHCONH	−0.55	0.43	>19	15	>12
63–66	4'	NHCONHCH ₂	−1.09	0.46	>31	16	>19
67–70	3'	OCONH	−0.75	0.059	1.6	0.31	0.37
72–75	4'	OCONH	−0.09	0.41	>22	15	>14
78–81	4'	OCONHCH ₂	−0.73	0.39	>12	14	>7.5

^aMean difference in CLogP values between compounds in the linker subclass X and the OCH₂-linked analogues having the same biaryl geometry (4' or 3' link) and bearing the same substituents. ^bRatio of mean MIC values (X/OCH₂) for the various linker subclasses; data for the parent series (*para*: MABA 0.028, LORA 1.6 μM ; *meta*: MABA 0.19, LORA 4.3 μM) were derived from refs 13 and 15 (see text).

Table 5. Comparative Activities of Mono- and Biphenyl Analogues: Influence of Overall Lipophilicity



comps		X	ΔCLogP^a	MIC (μM)				MIC ratio ^b (I/II)	
I	II			MABA		LORA		MABA	LORA
1	3	OCH ₂	1.84	0.50	0.035	2.6	1.3	14	2.0
22	39	NHCOCH ₂	1.84	0.27	0.22	21	5.0	1.2	4.2
23	44	NHCOCH ₂ O	1.67	0.16	0.18	10	25	0.89	0.40
28	49	NHCO ₂ CH ₂	1.84	0.15	0.11	11	5.0	1.4	2.2
29	59	NHCONH	1.92	0.23	0.06	4.2	18	3.8	0.23
32	65	NHCONHCH ₂	1.84	0.27	1.0	4.1	32	0.27	0.13
33	74	OCONH	2.24	0.12	0.05	2.7	>32	2.4	<0.084
35	80	OCONHCH ₂	1.84	0.25	0.52	17	2.4	0.48	7.1

^aDifference in CLogP values between compounds of forms I and II in each linker class. ^bRatio of MIC values (I/II) for mono- vs biphenyl compounds in each linker class.

as well. These results are illustrated graphically in Figure S1 (see Supporting Information). Thus, the *O*-carbamates **67–69** showed the best MIC profiles of all of the biaryl derivatives, comparable to **3**. However, a closer examination of the MIC results for the *para*-linked biaryl analogues having the latter two linkers (X = NHCONH and OCONH; compounds **57–60** and **72–75**) indicated that there was an unusually high variability in the MABA data across these sets (Table 3), with the very poorly active 4-F compounds (**58** and **73**, each tested 3–5 times) severely distorting the averages. Exclusion of these outliers led to mean MABA MIC values of 0.14 and 0.12 μM , respectively, essentially the same as for the *N*-linked carbamates (**47–50**), and with the 4-OCF₃ analogues (**59** and **74**) having useful aerobic potencies (0.05–0.06 μM) although very poor anaerobic activities.

Table 5 compares the MIC data for the 4-OCF₃ biphenyl compounds with those of the corresponding monophenyl analogues bearing the same linker groups. Despite an increase of 1.7–2.2 units in CLogP values for the biphenyl compounds, which in the OCH₂-linked series resulted in a 14-fold increase in MABA potency,¹³ in the present work the MIC values of the biphenyl series against replicating *M. tb* were scarcely improved

over those of their monoaryl congeners (and were poorer in some cases; see Figure S2 in Supporting Information). Potencies in the LORA assay were also generally similar or worse (see Figure S3 in Supporting Information). These results are reminiscent of those found for the previous study¹⁶ of extended ether linkers and are again consistent with a rather constrained hydrophobic binding domain in the activating nitroreductase that requires a very specific disposition of the larger biphenyl side chain for optimal interactions, which the alternative linkers may not allow.

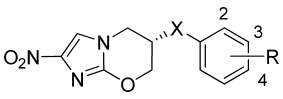
Because the biaryl compounds of Table 3 generally showed similar MIC potencies to the monoaryl compounds of Table 1 but were much less soluble, they demonstrate little apparent therapeutic advantage (at least *in vitro*). In a further attempt to utilize the favorable properties of the *O*-carbamate linker, a small set of aryl-terminating cyclic amine-based analogues was prepared and evaluated (Table 6). Similar side chains have previously been reported to be effective replacements for a biaryl substituent, with arylpiperazine being recognized as a bioisostere of the biaryl moiety.^{31–33} The obvious major potential benefit of such substitution is significantly improved aqueous solubility, and this was demonstrated here, with the 4-OCF₃

phenyl analogues (**82**, **83**, and **85**) showing comparable solubility values to **1** (at pH = 7), and the more hydrophilic pyridine derivative **84** being 5-fold better. Arylpiperazine **82** also displayed an excellent MIC profile (MABA 0.033 μM , LORA 1.1 μM), similar to that of the much more lipophilic and poorly soluble biphenyl analogue **3**, and aryloxypyrrolidine **83** was only slightly less impressive. In contrast, compounds **84** and **85** provided significantly reduced potencies, especially in the LORA (nonreplicating) assay.

Representative compounds bearing a variety of different linkers and with good MABA activity (IC_{50} values ranging from 0.03 to 0.25 μM) were subsequently evaluated for metabolic stability in human (HLM) and mouse liver microsomes

(MLM) as an indicator of suitability for in vivo evaluation (Table 7; comparative data for **1** and **3** are also provided).¹³ All of the compounds except *N*-methyl carbamate **34** showed notably high stabilities toward both HLM and MLM (>80% parent remaining after 1 h). However, examination of the metabolite profile of **34** showed only a single compound, the desmethyl carbamate **33**, which displayed excellent metabolic stability (superior to **1** in HLM). The biphenyl derivative of **33**, **74**, similarly demonstrated higher stability than the OCH_2 -linked analogue **3**, with negligible metabolism by either HLM or MLM occurring over the 1 h incubation period. Importantly, the more soluble arylpiperazine carbamate **82** (a bioisostere of **74**) was also acceptably stable (similar to **1** in HLM, though inferior to **74**).

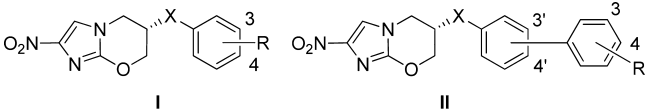
Table 6. Physicochemical Properties and MIC Values for Cyclic Amine Carbamate-Linked Analogues of 1



compd	X	R	CLogP ^a	solubility ^b	MIC ^c (μM)	
					MABA	LORA
82		4-OCF ₃	3.07	17	0.033 ± 0.019	1.1 ± 0.3
83		4-OCF ₃	3.21	21	0.06 ± 0.01	1.6 ± 0.1
84		3-aza, 4-CF ₃	2.10	94	0.14 ± 0.08	27 ± 7
85		4-OCF ₃	3.40	11	0.18 ± 0.08	26 ± 5

^aCLogP values, calculated using the ACD LogP/LogD prediction software (version 12.0, Advanced Chemistry Development Inc., Toronto, Canada). ^bSolubility ($\mu\text{g}/\text{mL}$) in water at pH = 7 and 20 °C, determined by HPLC (see Experimental Section). ^cMinimum inhibitory concentration, determined under aerobic (MABA)³⁰ or anaerobic (LORA)²⁸ conditions. Each value is the mean of at least two independent determinations ± SD.

Table 7. Microsomal Stability and in Vivo Efficacy Data for Selected Compounds



compd	form	X	R	solubility ^a	microsomes (% remaining at 1 h) ^b		in vivo efficacy (ratio vs 1 or 2)	
					H	M	acute ^c	chronic ^d
1	I	OCH ₂	4-OCF ₃	19	82	94	1.00	0.14
3	II	OCH ₂ (4')	4-OCF ₃	1.2	97	96	>205	0.86
33	I	OCONH	4-OCF ₃	5.4	88	89	0.39	0.02
34	I	OCON(Me)	4-OCF ₃	18	37	1 ^e	5.3	
36	I	OCH ₂ CONH	4-OCF ₃	68	100	85	0.33	
54	II	NHCONH (3')	4-OCF ₃	3.0	86	88	<0.01	
59	II	NHCONH (4')	4-OCF ₃	0.17	91	90	1.0	
69	II	OCONH (3')	4-OCF ₃	0.07	88	93	3.4	
70	II	OCONH (3')	3-aza, 4-CF ₃	5.8	89	80	0.02	
74	II	OCONH (4')	4-OCF ₃	0.06	100	98	5.0	0.35
82	I		4-OCF ₃	17	82	85	5.2	0.92 ^f

^aSolubility ($\mu\text{g}/\text{mL}$) in water at pH = 7 and 20 °C, determined by HPLC. ^bPooled human (H) or CD-1 mouse (M) liver microsomes. ^cFold reduction in lung CFUs for compound compared with the fold CFU reduction for **1** in a mouse model of acute TB infection (see text). ^dFold reduction in lung CFUs for compound compared with the fold CFU reduction for **2** in a mouse model of chronic TB infection (see text). ^eRapid metabolism to the desmethyl carbamate **33** was observed. ^fEight week study, dosing at 30 mg/kg.

Table 8. Pharmacokinetic Parameters for Selected Analogues in CD-1 Mice Following a Single Oral Dose of 40 mg/kg

compd	plasma			lung			AUC ratio ^b
	AUC _{0–inf} ^a (μg·h/mL)	C _{max} (μg/mL)	t _{1/2} (h)	AUC _{0–inf} ^a (μg·h/mL)	C _{max} (μg/mL)	t _{1/2} (h)	
3	198	7.4	14.4	218	9.0	12.8	1.1
4	296	12	24	81	18	2.2	0.27
33	28.5	1.4	9.8	43.3	3.8	4.1	1.5
59	6.61	0.48	6.3	>60	4.7	c	>9.0
74	44.9	0.52	62.3	>136	6.9	c	>3.0
82	53.4	2.5	10.5	169	11.7	10.5	3.2

^aArea under the curve, extrapolated to infinity. ^bLung AUC/plasma AUC. ^cNot calculable.

Table 9. Pharmacokinetic Parameters and Oral Bioavailability Data for 82 in Rats and Dogs

food type	intravenous ^a				oral (20 mg/kg)				
	C ₀ ^b (μg/mL)	T _{max} (h)	t _{1/2} (h)	AUC _{last} (μg·h/mL)	C _{max} (μg/mL)	T _{max} (h)	t _{1/2} (h)	AUC _{last} ^c (μg·h/mL)	F ^d (%)
normal	Rats (Sprague–Dawley)								
	0.70	0.083	8.3	5.93	4.4	5.0	e	67.4	57
normal high fat	Dogs (Beagle)								
	1.7	0.5	28	27.6	5.8	8.0	29	232	84
					5.2	12	30	182	

^aThe intravenous dose was 1 mg/kg for rats and 2 mg/kg for dogs. ^bMaximum plasma concentration extrapolated to $t = 0$. ^cArea under the curve calculated to the last time point; for rats the last time point was 24 h, while for dogs it was 72 h. ^dOral bioavailability, determined using dose normalized AUC_{last} values. ^eNot calculable.

Further confirmation of the metabolic stability of these urea and carbamate linkers was obtained from mouse pharmacokinetic studies on selected examples (Table 8). Here, the four compounds examined each showed good plasma half-lives (>6 h) and satisfactory exposure levels in lung tissue following oral dosing, but **82** possessed the best profile overall.

The compounds above were further assessed in an acute infection mouse tuberculosis model, measuring the fold reduction in colony-forming units (CFUs) in the lung following oral dosing at 100 mg/kg daily for 5 days per week over 3 weeks^{13,30} (Table 7). The fold reductions in CFUs were compared to that achieved with the OCH₂-linked compound **1**, which was employed as an internal reference standard in each of the experiments. In the monoaryl series, *N*-methyl carbamate **34** was unexpectedly found to be moderately better than **1** (5-fold), but its des-methyl metabolite **33** was less effective than **1** (consistent with a previous study of **33**²⁰). The greater efficacy for the *N*-methyl analogue (despite its poor stability) may in part be related to its 3-fold higher aqueous solubility (consistent with its lower CLogP value), which might allow better absorption and distribution. In contrast, the highly soluble ether-extended amide analogue **36** was no better than **33**. Figure S4 (in Supporting Information) illustrates these various solubility and in vivo efficacy effects. Examining the more lipophilic biaryl series, poorly soluble *O*-carbamates **69** and **74** (respectively 3.4- and 5-fold better than **1**) were superior to the corresponding urea analogues, **54** and **59**, with the *para*-linked examples having better efficacies than their *meta*-linked counterparts, in agreement with previous studies.^{15,16} While the biaryl carbamate **74** was found to be 13-fold more efficacious than the monoaryl analogue **33**, it is worth noting that this is significantly less than the more than 205-fold improvement seen for OCH₂-linked biphenyl analogue **3** over **1**, confirming the superiority of the OCH₂-linker for high in vivo efficacy, as previously observed.^{13–16} An attempt to improve aqueous solubility using trifluoromethylpyridine as a replacement for the terminal aryl ring^{14–16} (**70**) concomitantly abolished the in vivo activity. In contrast, the arylpiperazine carbamate **82**

demonstrated equivalent in vivo efficacy to its bioisostere **74** (5.2-fold better than **1**) and showed a 283-fold higher aqueous solubility than biaryl **74** at pH = 7 (4083-fold higher at pH = 1, consistent with its calculated pK_a value of 2.44).

These interesting results prompted a further appraisal of the antitubercular activities of *O*-carbamates **33**, **74**, and **82** in a more stringent chronic disease mouse model (Table 7), where the infection was first established for ~50–70 days (resulting in a growth plateau) prior to daily oral dosing (for 5 days per week over 3–8 weeks).¹⁵ Compared to the clinical trial drug **2** (an order of magnitude more efficacious than **1** in this assay), monophenyl carbamate **33** was almost completely ineffective, while its biaryl derivative **74** was weakly active (0.35-fold, but ~3-fold superior to **1**). Intriguingly, despite its fairly modest activity in the acute in vivo assay, the arylpiperazine carbamate **82** displayed essentially equivalent efficacy to both **2** and **3** in this chronic model and was much more soluble than both compounds (>1000-fold at pH = 7.4 in a thermodynamic solubility assay); therefore **82** was selected for advanced studies.

Additional pharmacokinetic data for **82** in the rat (see Table 9) may be compared to previously reported data for pyridine **4**.¹⁵ While **4** gave a higher maximum plasma concentration following oral dosing (8.1 versus 4.4 μg/mL), both compounds provided similar oral bioavailabilities (**4**, 62%; **82**, 57%). Moreover, a re-examination of the mouse pharmacokinetic data (Table 8) revealed that **82** afforded a more prolonged exposure than **4** in the lung (the primary infection site). A further study of **82** was then conducted in dogs to ascertain the effect of diet on the pharmacokinetic profile observed. Knowledge about the influence of food is important in the treatment of tuberculosis, where the drugs are taken once daily or less; among the first line agents, isoniazid shows reduced bioavailability with food.³⁴ Dietary fat commonly increases the absorption of less bioavailable lipophilic drugs by improving their dissolution, but hydrophilic drugs are not significantly affected.³⁵ The results (Table 9) show that **82** has excellent oral bioavailability in dogs (84%), providing

high exposures and a long half-life (29 h) that are not markedly altered by a high fat diet.

With the attrition of new drug candidates in clinical trials estimated at 95%, it has been recommended that chemists pay greater attention to fundamental compound properties that can help to predict fitness for survival as potential drugs, rather than focusing too much on potency alone.³⁶ Whereas issues of pharmacokinetics and bioavailability were historically the major reasons for drug failure, other factors, such as toxicology and clinical safety, as well as efficacy, are now more predominant.³⁶ There is increasing recognition that high molecular weight and high lipophilicity are associated not only with poor oral drug-like properties (particularly low solubility) but also with a higher risk of observing toxicity or unwanted side effects.³⁷ Thus CLogP values of between 2 and 3 are often considered optimal for oral drugs, and although better antitubercular activity has been observed in several studies for somewhat more lipophilic compounds (CLogP ~4), the majority of current TB drugs still have LogP values ranging from 2.5 to 4.³⁸ With this in mind, we obtained further physical and safety data for **82** and compared these with results for the parent clinical trial agent **1** (Table 10). While **82** has a higher molecular weight than **1**

Table 10. Additional Comparative Data for **1 and **82****

property	1	82
molecular weight (Da)	359.3	457.4
log P_{exp}	2.52 ± 0.02	2.82 ± 0.03
thermodynamic solubility (μM):		
pH = 7.4	30	33
pH = 1	30	169
human plasma protein binding (%)	94 ^a	91
mutagenic effect (Ames test)	no	no ^b

^aReference 39. ^bNot mutagenic up to precipitating concentrations (>75 $\mu\text{g}/\text{well}$) in strains TA98 and TA100, both in the presence and absence of metabolic activation (S9 fraction).

(457 versus 359), the measured LogP results for these compounds were comparable (2.82 versus 2.52), as were their thermodynamic solubility values at pH = 7.4 (30–33 μM); compound **82** was also about 6-fold more soluble than **1** at low pH (0.17 mM). Moreover, **82** displayed a reduced binding to human plasma proteins (91% versus 94% for **1**³⁹), which together with its very low inhibition of hERG (IC_{50} >30 μM) suggested an improved potential for safety.⁴⁰ Finally, we confirmed that (like **1**) carbamate **82** did not show any mutagenic effect (Ames test, *Salmonella* tester strains TA98 and TA100, conducted with and without metabolic activation).

CONCLUSIONS

The current investigation set out to evaluate various amide, carbamate, and urea linkers as possible replacements for the OCH_2 linkage of **1** in order to address oxidative metabolism, minimize compound lipophilicity, and enhance aqueous solubility, with the overall aim of improved safety. The new compounds were generally more hydrophilic than the OCH_2 linked analogues, as assessed by CLogP values, and many of the monoaryl analogues tested (particularly those having amide or urea linkers) offered solubility increases, compared to **1** itself. Extended amide, *N*- or *O*-carbamate monoaryl derivatives provided moderately improved aerobic potencies (but reduced anaerobic activity), urea analogues a more balanced MIC profile (similar to the 6-amino analogue of **1**), while the

(nonextended) *O*-carbamate analogue of **1** (**33**) proved to be the best and displayed high microsomal stability.

These encouraging findings prompted combination of some of the linkers together with particular biaryl side chains that had been proven to greatly enhance both in vitro and (notably) in vivo activity in the parent (OCH_2 linked) series. However, the resulting biaryl compounds were generally not greater in potency than their monoaryl counterparts. Furthermore, only for *meta*-linked examples were the urea and carbamate linkers superior to OCH_2 , reinforcing previous conclusions regarding structural limitations for preferred binding to the activating nitroreductase.^{16,21} Nevertheless, upon further evaluation in a mouse model of acute *M. tb* infection, the highly stable *para*-linked biaryl (*O*-)carbamate **74** was found to be superior to both the leading monoaryl analogue **33** (13-fold) and the parent drug **1** (5-fold), although it was very poorly soluble. A consideration of possible biaryl replacements in this most promising (*O*-carbamate) series led to the potent, more hydrophilic arylpiperazine analogue **82**, a bioisostere of biaryl carbamate **74**. This compound provided equivalent in vivo efficacy to the latter in the acute in vivo model but was as soluble as **1** at neutral pH (and 5.6-fold more soluble than **1** at low pH). Carbamate **82** additionally provided a similar level of in vivo efficacy to the clinical trial drug **2** in a more stringent chronic infection model (with greatly superior aqueous solubility over **2**) and compared well to the parent drug **1** in other respects (e.g., reduced binding to human plasma proteins). Pharmacokinetic assessments of **82** across several species also revealed favorable profiles, including high oral bioavailabilities and minimal food effects, suggesting that this compound may be worthy of further study.

EXPERIMENTAL SECTION

Combustion analyses were performed by the Campbell Micro-analytical Laboratory, University of Otago, Dunedin, New Zealand. Melting points were determined using an Electrothermal IA9100 melting point apparatus and are as read. NMR spectra were measured on a Bruker Avance 400 spectrometer at 400 MHz for ^1H and are referenced to Me_4Si . Chemical shifts and coupling constants are recorded in units of ppm and hertz, respectively. High-resolution electron impact (HREIMS) and fast atom bombardment (HRFABMS) mass spectra were determined on a VG-70SE mass spectrometer at nominal 5000 resolution. High-resolution electrospray ionization (HRESIMS) mass spectra were determined on a Bruker micrOTOF-Q II mass spectrometer. Low-resolution atmospheric pressure chemical ionization (APCI) mass spectra were measured for organic solutions on a ThermoFinnigan Surveyor MSQ mass spectrometer, connected to a Gilson autosampler. Thin-layer chromatography was carried out on aluminum-backed silica gel plates (Merck 60 F_{254}), with visualization of components by UV light (254 nm) or exposure to I_2 . Column chromatography was carried out on silica gel (Merck 230–400 mesh). Compounds of Tables 1, 3, and 6 were isolated following trituration in Et_2O (or $\text{CH}_2\text{Cl}_2/\text{Et}_2\text{O}$) unless otherwise indicated. HPLC determinations of purity were conducted on an Agilent 1100 system using a reversed phase C8 column with diode array detection.

Compounds of Table 1. Procedure A: (6*S*)-2-Nitro-6-[[2-(trifluoromethoxy)benzyl]oxy]-6,7-dihydro-5*H*-imidazo[2,1-*b*][1,3]-oxazine (**8**) (Scheme 1A). 1-(Bromomethyl)-2-(trifluoromethoxy)-benzene (105 μL , 0.65 mmol) and NaH (30 mg of 60% dispersion in mineral oil, 0.75 mmol) were successively added to a solution of (6*S*)-2-nitro-6,7-dihydro-5*H*-imidazo[2,1-*b*][1,3]oxazin-6-ol²⁰ (**6**) (100 mg, 0.54 mmol) in anhydrous DMF (3 mL). The mixture was stirred at 20 °C for 2.5 h and then diluted with EtOAc (150 mL) and washed with water. The aqueous layer was re-extracted with EtOAc, and the combined organic layers were washed with brine, dried (Na_2SO_4), and concentrated under reduced pressure. The residue was chromatographed

on silica gel, eluting with a gradient of 0–4% MeOH/CH₂Cl₂, to give **8**²² (135 mg, 70%) as a white solid: mp 108–110 °C. ¹H NMR [(CD₃)₂SO] δ 8.02 (s, 1 H), 7.51 (dd, *J* = 7.4, 1.8 Hz, 1 H), 7.45 (dd, *J* = 7.8, 1.9 Hz, 1 H), 7.41–7.33 (m, 2 H), 4.72 (s, 2 H), 4.66 (dt, *J* = 12.1, 2.4 Hz, 1 H), 4.49 (d, *J* = 11.7 Hz, 1 H), 4.32–4.21 (m, 3 H). Anal. (C₁₄H₁₂F₃N₃O₅) C, H, N.

Procedure B: *N*-[(6*S*)-2-Nitro-6,7-dihydro-5*H*-imidazo[2,1-*b*][1,3]-oxazin-6-yl]-2-(trifluoromethoxy)benzamide (**10**) (Scheme 2A). 2-(Trifluoromethoxy)benzoyl chloride (140 mg, 0.623 mmol) and DIPEA (200 μL, 1.15 mmol) were successively added to a solution of (6*S*)-2-nitro-6,7-dihydro-5*H*-imidazo[2,1-*b*][1,3]oxazin-6-amine hydrochloride²⁰ (**91**) (101 mg, 0.458 mmol) in anhydrous DMF (3 mL). The mixture was stirred at 20 °C for 1 h and then diluted with EtOAc (200 mL) and washed with saturated aqueous NaHCO₃ and brine. The aqueous layer was re-extracted with EtOAc, and the combined organic layers were dried (Na₂SO₄) and concentrated under reduced pressure. The residue was chromatographed on silica gel, eluting with a gradient of 0–4% MeOH/CH₂Cl₂, to give **10** (140 mg, 82%) as a white solid: mp 172–174 °C. ¹H NMR [(CD₃)₂SO] δ 9.08 (d, *J* = 6.5 Hz, 1 H), 8.09 (s, 1 H), 7.62–7.54 (m, 2 H), 7.49–7.40 (m, 2 H), 4.64–4.58 (m, 1 H), 4.56 (dd, *J* = 11.2, 2.1 Hz, 1 H), 4.45 (ddd, *J* = 11.2, 3.8, 1.8 Hz, 1 H), 4.39 (dd, *J* = 13.0, 4.8 Hz, 1 H), 4.09 (ddd, *J* = 13.0, 2.9, 1.8 Hz, 1 H). Anal. (C₁₄H₁₁F₃N₄O₅·0.5H₂O) C, H, N.

Procedure C: *N*-Methyl-*N*-[(6*S*)-2-nitro-6,7-dihydro-5*H*-imidazo[2,1-*b*][1,3]oxazin-6-yl]-2-(trifluoromethoxy)benzamide (**13**). A solution of amide **10** (48 mg, 0.13 mmol) in anhydrous DMF (1 mL) at 0 °C was successively treated with NaH (12 mg of 60%, 0.30 mmol) and MeI (12 μL, 0.19 mmol). The mixture was stirred at 0 °C for 90 min and then water (100 mL) was added and the product was extracted with EtOAc (3 × 100 mL). The combined extracts were washed with brine, dried (Na₂SO₄), and concentrated under reduced pressure. The residue was chromatographed on silica gel, eluting with a gradient of 0–4% MeOH/CH₂Cl₂, to give **13** (39 mg, 78%) as a white solid: mp 187–190 °C. ¹H NMR [(CD₃)₂SO] δ 8.13 (s, 1 H), 7.64–7.45 (m, 4 H), 5.10–5.01 (m, 1 H), 4.75–4.60 (m, 2 H), 4.47–4.26 (m, 2 H), 2.73 (s, 3 H). Anal. (C₁₅H₁₃F₃N₄O₅) C, H, N.

N-[(6*S*)-2-Nitro-6,7-dihydro-5*H*-imidazo[2,1-*b*][1,3]oxazin-6-yl]-2-(trifluoromethoxy)benzenesulfonamide (**16**). Reaction of amine salt **91** with 2-(trifluoromethoxy)benzenesulfonyl chloride (1.25 equiv) and DIPEA, using procedure B, gave **16** (83%) as a white solid: mp 214–219 °C. ¹H NMR [(CD₃)₂SO] δ 8.83 (br s, 1 H), 7.99 (s, 1 H), 7.98–7.93 (m, 1 H), 7.83–7.78 (m, 1 H), 7.62–7.56 (m, 2 H), 4.43 (dd, *J* = 11.3, 2.1 Hz, 1 H), 4.30 (ddd, *J* = 11.3, 4.5, 1.7 Hz, 1 H), 4.25 (dd, *J* = 12.9, 4.6 Hz, 1 H), 4.08 (br s, 1 H), 3.98 (ddd, *J* = 12.9, 3.7, 1.7 Hz, 1 H). Anal. (C₁₅H₁₁F₃N₄O₆S) C, H, N.

Procedure D: *N*-Methyl-*N*-[(6*S*)-2-nitro-6,7-dihydro-5*H*-imidazo[2,1-*b*][1,3]oxazin-6-yl]-2-(trifluoromethoxy)benzenesulfonamide (**19**). A solution of sulfonamide **16** (75 mg, 0.18 mmol) in anhydrous DMF (2 mL) was successively treated with K₂CO₃ (77 mg, 0.56 mmol) and MeI (23 μL, 0.37 mmol). The mixture was stirred at 20 °C for 2 h and then diluted with EtOAc (200 mL) and washed with saturated aqueous NaHCO₃ and brine. The aqueous layer was re-extracted with EtOAc, and the combined organic layers were dried (Na₂SO₄) and concentrated under reduced pressure. The residue was chromatographed on silica gel, eluting with a gradient of 0–4% MeOH/CH₂Cl₂, to give **19** (70 mg, 90%) as a white solid: mp 160–162 °C. ¹H NMR [(CD₃)₂SO] δ 8.03 (dd, *J* = 7.8, 1.7 Hz, 1 H), 8.03 (s, 1 H), 7.89–7.84 (m, 1 H), 7.68–7.64 (m, 1 H), 7.62 (dt, *J* = 7.7, 1.0 Hz, 1 H), 4.59–4.51 (m, 2 H), 4.47–4.40 (m, 1 H), 4.29–4.18 (m, 2 H), 2.83 (s, 3 H). Anal. (C₁₄H₁₃F₃N₄O₆S) C, H, N.

Procedure E: 2-[(6*S*)-2-Nitro-6,7-dihydro-5*H*-imidazo[2,1-*b*][1,3]-oxazin-6-yl]amino-1-[4-(trifluoromethoxy)phenyl]ethanone (**25**) (Scheme 2D). 2-Bromo-1-[4-(trifluoromethoxy)phenyl]ethanone (157 mg, 0.555 mmol) and DIPEA (200 μL, 1.15 mmol) were successively added to a solution of amine salt **91** (103 mg, 0.467 mmol) in anhydrous DMF (2 mL). The mixture was stirred at 20 °C for 2.5 h, and then brine (100 mL) was added and the product was extracted with EtOAc (3 × 150 mL). The combined extracts were washed with brine, dried (Na₂SO₄), and concentrated under reduced pressure. The residue was chromatographed on silica gel, eluting with a gradient of 0–2% MeOH/CH₂Cl₂, to give **25** (11 mg, 6%) as a

light-yellow solid: mp 120–124 °C. ¹H NMR (CDCl₃) δ 8.01–7.97 (m, 2 H), 7.42 (s, 1 H), 7.33 (br d, *J* = 8.0 Hz, 2 H), 4.48–4.36 (m, 2 H), 4.28–4.17 (m, 3 H), 3.97 (ddd, *J* = 12.3, 5.2, 1.2 Hz, 1 H), 3.49–3.43 (m, 1 H), 2.30 (br s, 1 H). HRFABMS calcd for C₁₅H₁₄F₃N₄O₅ *m/z* [M + H]⁺ 387.0916, found 387.0913. HPLC purity: 93.2%.

Procedure F: 4-(Trifluoromethoxy)phenyl [(6*S*)-2-nitro-6,7-dihydro-5*H*-imidazo[2,1-*b*][1,3]oxazin-6-yl]carbamate (**27**) (Scheme 3A). 4-(Trifluoromethoxy)phenol (65 μL, 0.50 mmol) and DIPEA (90 μL, 0.52 mmol) were successively added to a solution of triphosgene (77 mg, 0.25 mmol) in anhydrous CH₂Cl₂ (2 mL) at 0 °C. The mixture was stirred at 0–20 °C for 4 h to give a solution of the crude aryl chloroformate. A solution of amine salt **91** (86 mg, 0.39 mmol) and DIPEA (175 μL, 1.00 mmol) in anhydrous CH₂Cl₂ (3 mL) was then added, and the mixture was stirred at 20 °C for a further 90 min. Following dilution with EtOAc (200 mL), the solution was washed with saturated aqueous NaHCO₃ and brine. The aqueous layer was re-extracted with EtOAc and the combined organic layers were dried (Na₂SO₄) and concentrated under reduced pressure. The residue was chromatographed on silica gel, eluting with a gradient of 0–4% MeOH/CH₂Cl₂, to give **27** (60 mg, 40%) as an off-white solid: mp 177–179 °C. ¹H NMR [(CD₃)₂SO] δ 8.58 (d, *J* = 6.2 Hz, 1 H), 8.08 (s, 1 H), 7.40 (d, *J* = 8.6 Hz, 2 H), 7.28 (d, *J* = 9.0 Hz, 2 H), 4.56–4.42 (m, 2 H), 4.36 (dd, *J* = 12.8, 4.7 Hz, 1 H), 4.32–4.24 (m, 1 H), 4.15–4.08 (m, 1 H). Anal. (C₁₄H₁₁F₃N₄O₆) C, H, N.

1-[(6*S*)-2-Nitro-6,7-dihydro-5*H*-imidazo[2,1-*b*][1,3]oxazin-6-yl]-3-[4-(trifluoromethoxy)phenyl]urea (**29**) (Scheme 3B). A mixture of the free base of amine salt **91** (50 mg, 0.27 mmol) and 1-isocyanato-4-(trifluoromethoxy)benzene (50 μL, 0.33 mmol) in anhydrous DMF (2 mL) was stirred at 20 °C for 5 h. Brine (100 mL) was then added, and the product was extracted with EtOAc (3 × 100 mL). The combined extracts were washed with brine, dried (Na₂SO₄), and concentrated under reduced pressure. The residue was chromatographed on silica gel, eluting with a gradient of 0–2% MeOH/CH₂Cl₂, to give **29**²⁰ (14 mg, 13%) as a light-yellow solid: mp 166 °C (dec). ¹H NMR [(CD₃)₂SO] δ 8.61 (s, 1 H), 8.09 (s, 1 H), 7.49–7.44 (m, 2 H), 7.23 (br d, *J* = 8.4 Hz, 2 H), 6.91 (d, *J* = 6.8 Hz, 1 H), 4.56 (dd, *J* = 11.2, 1.9 Hz, 1 H), 4.45 (ddd, *J* = 11.2, 3.3, 2.0 Hz, 1 H), 4.41–4.35 (m, 1 H), 4.30 (dd, *J* = 12.8, 4.1 Hz, 1 H), 4.10 (dt, *J* = 12.8, 2.2 Hz, 1 H). HRFABMS calcd for C₁₄H₁₃F₃N₅O₅ *m/z* [M + H]⁺ 388.0869, found 388.0862. HPLC purity: 95.1%.

Procedure G: 1-[(6*S*)-2-Nitro-6,7-dihydro-5*H*-imidazo[2,1-*b*][1,3]-oxazin-6-yl]-3-[4-(trifluoromethoxy)phenyl]thiourea (**31**). A solution of amine salt **91** (101 mg, 0.458 mmol) and NMM (100 μL, 0.91 mmol) in anhydrous DMF (2 mL) was successively treated with 1-isothiocyanato-4-(trifluoromethoxy)benzene (110 μL, 0.68 mmol) and dibutyltin diacetate (3 drops). The mixture was stirred at 20 °C for 2 h, then diluted with EtOAc (150 mL) and washed with brine. The aqueous layer was re-extracted with EtOAc, and the combined organic layers were washed with brine, dried (Na₂SO₄), and concentrated under reduced pressure. The residue was chromatographed on silica gel, eluting with a gradient of 0–2% MeOH/CH₂Cl₂, to give **31** (32 mg, 17%) as a cream solid: mp (CH₂Cl₂/hexane) 178 °C (dec). ¹H NMR (CDCl₃) δ 8.43 (d, *J* = 8.6 Hz, 1 H), 8.36 (s, 1 H), 7.44–7.39 (m, 2 H), 7.21 (s, 1 H), 7.13 (d, *J* = 8.3 Hz, 2 H), 5.65–5.59 (m, 1 H), 4.87 (dt, *J* = 11.7, 2.0 Hz, 1 H), 4.45 (dd, *J* = 11.6, 1.5 Hz, 1 H), 4.32–4.20 (m, 2 H). Anal. (C₁₄H₁₃F₃N₅O₄S·0.25EtOAc) C, H, N.

Procedure H: (6*S*)-2-Nitro-6,7-dihydro-5*H*-imidazo[2,1-*b*][1,3]-oxazin-6-yl [4-(trifluoromethoxy)phenyl]carbamate (**33**) (Scheme 1A). 1-Isocyanato-4-(trifluoromethoxy)benzene (1.50 mL, 9.94 mmol) and CuCl (95 mg, 0.96 mmol) were successively added to a solution of alcohol **6** (1.50 g, 8.10 mmol) in anhydrous DMF (20 mL). The mixture was stirred at 20 °C for 3 h and then diluted with EtOAc (150 mL) and washed with 0.2 N HCl, water, and brine. The aqueous layer was re-extracted with EtOAc and the combined extracts were dried (Na₂SO₄) and concentrated under reduced pressure. The residue was chromatographed on silica gel, eluting with a gradient of 0–2% MeOH/CH₂Cl₂, to give **33**²⁰ (2.50 g, 80%) as a white solid: mp 211–213 °C [lit.²⁰ 220 °C (dec)]. ¹H NMR [(CD₃)₂SO] δ 10.08 (s, 1 H), 8.08 (s, 1 H), 7.56 (d, *J* = 8.8 Hz, 2 H), 7.30 (d, *J* = 8.4 Hz, 2 H),

5.44 (br s, 1 H), 4.64 (br s, 2 H), 4.45–4.40 (m, 1 H), 4.35–4.30 (m, 1 H). Anal. (C₁₄H₁₁F₃N₄O₆·0.25Et₂O) C, H, N. HPLC purity: 100%.

2-[[*(6S)*-2-Nitro-6,7-dihydro-5H-imidazo[2,1-*b*][1,3]oxazin-6-yl]-oxy]-*N*-[4-(trifluoromethoxy)phenyl]acetamide (**36**). Reaction of alcohol **6** with 2-chloro-*N*-[4-(trifluoromethoxy)phenyl]acetamide and NaH (1.55 equiv), using procedure A (but at 0–20 °C for 6 h), gave **36**²² (19%) as a white solid: mp (CH₂Cl₂/petroleum ether) 73–76 °C. ¹H NMR (CDCl₃) δ 8.10 (s, 1 H), 7.58–7.54 (m, 2 H), 7.46 (s, 1 H), 7.19 (d, *J* = 8.4 Hz, 2 H), 4.74–4.68 (m, 1 H), 4.42 (d, *J* = 12.5 Hz, 1 H), 4.36–4.25 (m, 5 H). Anal. (C₁₅H₁₃F₃N₄O₆·0.25EtOAc) C, H, N. HPLC purity: 96.8%.

Compounds of Table 3. Procedure I. General Method for Suzuki Couplings. A stirred mixture of aryl-bromide or aryl-iodide (0.19 mmol) and arylboronic acid (or pinacol ester derivative) (0.25 mmol) in toluene (5 mL), EtOH (3 mL) and 2 M K₂CO₃ (1 mL) was purged with N₂ for 5 min. Pd(dppf)Cl₂ (9 μmol) was added, and the stirred mixture was heated under reflux in an N₂ atmosphere for 1 h (or until the reaction was complete). After cooling to 20 °C, the mixture was diluted with EtOAc (150 mL) and washed with water. The aqueous layer was re-extracted with EtOAc, and the combined organic layers were washed with brine, dried (Na₂SO₄), and concentrated under reduced pressure. The residue was chromatographed on silica gel, eluting with a gradient of 0–4% MeOH/CH₂Cl₂, to give the required products.

2-(4-Bromophenyl)-*N*-[[*(6S)*-2-nitro-6,7-dihydro-5H-imidazo[2,1-*b*][1,3]oxazin-6-yl]acetamide (**92**) (Scheme 2B). Reaction of amine salt **91** with (4-bromophenyl)acetyl chloride (1.5 equiv) and DIPEA, using procedure B for 3 h, gave **92** (83%) as a light-yellow solid: mp 199 °C (dec). ¹H NMR [(CD₃)₂SO] δ 8.70 (d, *J* = 6.4 Hz, 1 H), 8.08 (s, 1 H), 7.49–7.44 (m, 2 H), 7.21–7.16 (m, 2 H), 4.50–4.45 (m, 1 H), 4.41–4.32 (m, 2 H), 4.29 (dd, *J* = 12.9, 4.6 Hz, 1 H), 4.00 (dt, *J* = 12.9, 2.4 Hz, 1 H), 3.44 (s, 2 H). Anal. (C₁₄H₁₃BrN₄O₄) C, H, N.

N-[[*(6S)*-2-Nitro-6,7-dihydro-5H-imidazo[2,1-*b*][1,3]oxazin-6-yl]-2-[4'-(trifluoromethyl)biphenyl-4-yl]acetamide (**37**). Reaction of bromide **92** and 4-(trifluoromethyl)phenylboronic acid, using procedure I, gave **37** (62%) as a light-brown solid: mp 178–182 °C. ¹H NMR [(CD₃)₂SO] δ 8.74 (d, *J* = 6.3 Hz, 1 H), 8.09 (s, 1 H), 7.87 (d, *J* = 8.3 Hz, 2 H), 7.80 (d, *J* = 8.3 Hz, 2 H), 7.66 (d, *J* = 8.3 Hz, 2 H), 7.37 (d, *J* = 8.3 Hz, 2 H), 4.51 (br d, *J* = 9.2 Hz, 1 H), 4.45–4.35 (m, 2 H), 4.30 (dd, *J* = 12.9, 4.4 Hz, 1 H), 4.03 (dt, *J* = 12.9, 2.3 Hz, 1 H), 3.53 (s, 2 H). Anal. (C₂₁H₁₇F₃N₄O₄·0.25H₂O) C, H, N.

4-Iodobenzyl [[*(6S)*-2-nitro-6,7-dihydro-5H-imidazo[2,1-*b*][1,3]oxazin-6-yl]carbamate (**94**) (Scheme 3A). Reaction of triphosgene, 4-iodobenzyl alcohol, and DIPEA for 2 h, followed by reaction of the crude aryl chloroformate with amine salt **91** (1.0 equiv) and DIPEA for 3 h, using procedure F, gave **94** (43%) as an off-white solid: mp 204–208 °C. ¹H NMR [(CD₃)₂SO] δ 8.04 (s, 1 H), 8.01 (br d, *J* = 5.7 Hz, 1 H), 7.75–7.71 (m, 2 H), 7.19–7.14 (m, 2 H), 5.01 (s, 2 H), 4.46 (dd, *J* = 11.2, 2.1 Hz, 1 H), 4.37 (dd, *J* = 11.2, 2.8 Hz, 1 H), 4.29 (dd, *J* = 12.8, 4.7 Hz, 1 H), 4.23–4.16 (m, 1 H), 4.05–3.97 (m, 1 H). Anal. (C₁₄H₁₃I₂N₄O₅) C, H, N.

4'-(Trifluoromethyl)biphenyl-4-ylmethyl [[*(6S)*-2-nitro-6,7-dihydro-5H-imidazo[2,1-*b*][1,3]oxazin-6-yl]carbamate (**47**). Reaction of iodide **94** and 4-(trifluoromethyl)phenylboronic acid, using procedure I, gave **47** (77%) as a light-brown solid: mp 189–191 °C. ¹H NMR [(CD₃)₂SO] δ 8.05 (s, 1 H), 8.03 (d, *J* = 4.9 Hz, 1 H), 7.90 (br d, *J* = 8.2 Hz, 2 H), 7.81 (br d, *J* = 8.3 Hz, 2 H), 7.74 (d, *J* = 8.3 Hz, 2 H), 7.49 (br d, *J* = 8.0 Hz, 2 H), 5.13 (s, 2 H), 4.48 (dd, *J* = 11.2, 2.1 Hz, 1 H), 4.39 (dd, *J* = 11.2, 2.9 Hz, 1 H), 4.31 (dd, *J* = 12.7, 4.7 Hz, 1 H), 4.26–4.18 (m, 1 H), 4.07–4.00 (m, 1 H). Anal. (C₂₁H₁₇F₃N₄O₅) C, H, N.

1-(3-Bromophenyl)-3-[[*(6S)*-2-nitro-6,7-dihydro-5H-imidazo[2,1-*b*][1,3]oxazin-6-yl]urea (**95**) (Scheme 3B). Reaction of amine salt **91** and NMM with 1-bromo-3-isocyanatobenzene and dibutyltin diacetate, using procedure G for 4 h, gave **95** (92%) as a white solid: mp 160–165 °C. ¹H NMR [(CD₃)₂SO] δ 8.59 (s, 1 H), 8.08 (s, 1 H), 7.80–7.78 (m, 1 H), 7.22–7.15 (m, 2 H), 7.12–7.07 (m, 1 H), 6.94 (d, *J* = 6.7 Hz, 1 H), 4.56 (dd, *J* = 11.2, 2.0 Hz, 1 H), 4.45 (ddd, *J* = 11.2, 3.4, 2.0 Hz, 1 H), 4.39–4.33 (m, 1 H), 4.30 (dd, *J* = 12.7, 4.1 Hz, 1 H), 4.11 (dt, *J* = 12.7, 2.3 Hz, 1 H). Anal. (C₁₃H₁₂BrN₅O₄) C, H, N.

1-[[*(6S)*-2-Nitro-6,7-dihydro-5H-imidazo[2,1-*b*][1,3]oxazin-6-yl]-3-[4'-(trifluoromethyl)biphenyl-3-yl]urea (**52**). Reaction of bromide **95** and 4-(trifluoromethyl)phenylboronic acid, using procedure I, gave **52** (72%) as a brown solid: mp (EtOAc/petroleum ether) 156 °C (dec). ¹H NMR [(CD₃)₂SO] δ 8.57 (s, 1 H), 8.10 (s, 1 H), 7.81 (s, 5 H), 7.39–7.35 (m, 2 H), 7.31–7.26 (m, 1 H), 6.93 (d, *J* = 6.8 Hz, 1 H), 4.58 (dd, *J* = 11.2, 1.8 Hz, 1 H), 4.47 (ddd, *J* = 11.2, 3.3, 1.9 Hz, 1 H), 4.42–4.35 (m, 1 H), 4.31 (dd, *J* = 12.7, 4.1 Hz, 1 H), 4.13 (dt, *J* = 12.7, 2.2 Hz, 1 H). Anal. (C₂₀H₁₆F₃N₅O₄·0.5H₂O) C, H, N.

(6S)-2-Nitro-6,7-dihydro-5H-imidazo[2,1-*b*][1,3]oxazin-6-yl (3-bromophenyl)carbamate (**86**) (Scheme 1A). Reaction of alcohol **6** with 1-bromo-3-isocyanatobenzene and CuCl, using procedure H for 2.5 h, gave **86** (80%) as a white solid: mp 226 °C (dec). ¹H NMR [(CD₃)₂SO] δ 10.08 (s, 1 H), 8.07 (s, 1 H), 7.75 (br s, 1 H), 7.41 (br d, *J* = 7.8 Hz, 1 H), 7.25 (t, *J* = 7.9 Hz, 1 H), 7.20 (dt, *J* = 7.9, 1.5 Hz, 1 H), 5.44 (q, *J* = 1.6 Hz, 1 H), 4.65 (s, 2 H), 4.43 (dd, *J* = 14.0, 3.4 Hz, 1 H), 4.34 (dd, *J* = 14.0, 1.3 Hz, 1 H). Anal. (C₁₃H₁₁BrN₄O₅) C, H, N.

(6S)-2-Nitro-6,7-dihydro-5H-imidazo[2,1-*b*][1,3]oxazin-6-yl 4'-(trifluoromethyl)biphenyl-3-yl]carbamate (**67**). Reaction of bromide **86** and 4-(trifluoromethyl)phenylboronic acid, using procedure I, gave **67** (58%) as a cream solid: mp 125–128 °C. ¹H NMR [(CD₃)₂SO] δ 10.03 (s, 1 H), 8.09 (s, 1 H), 7.89–7.76 (m, 5 H), 7.54–7.47 (m, 1 H), 7.43 (t, *J* = 7.7 Hz, 1 H), 7.38 (dt, *J* = 7.6, 1.4 Hz, 1 H), 5.46 (br d, *J* = 1.4 Hz, 1 H), 4.66 (s, 2 H), 4.45 (dd, *J* = 13.9, 3.4 Hz, 1 H), 4.35 (d, *J* = 13.9 Hz, 1 H). Anal. (C₂₀H₁₅F₃N₄O₅) C, H, N.

Compounds of Table 6. Procedure J: *(6S)*-2-Nitro-6,7-dihydro-5H-imidazo[2,1-*b*][1,3]oxazin-6-yl 4-[4-(trifluoromethoxy)phenyl]piperazine-1-carboxylate (82**) (Scheme 4C).** Triphosgene (3.05 g, 10.3 mmol) was added in portions over 20 min to a stirred suspension of alcohol **6** (3.81 g, 20.6 mmol) and Et₃N (8.60 mL, 61.7 mmol) in anhydrous THF (120 mL) at 5 °C, such that the temperature of the mixture remained below 10 °C. After 10 min, the cooling bath was removed and the mixture was stirred at 20 °C for 90 min. A solution of 1-[4-(trifluoromethoxy)phenyl]piperazine²⁶ (**113**) (5.32 g, 21.6 mmol) in THF (20 mL) was added, and stirring was continued for another 2 h. Water was added, and the mixture was extracted with EtOAc. Evaporation of this extract gave an oily solid, which was chromatographed on silica gel. Elution with CH₂Cl₂ gave foreruns, and then further elution with 50% EtOAc/CH₂Cl₂ gave **82** (5.68 g, 62%) as a light-yellow solid: mp 166–168 °C. ¹H NMR [(CD₃)₂SO] δ 8.06 (s, 1 H), 7.19 (d, *J* = 9.0 Hz, 2 H), 6.99 (d, *J* = 9.0 Hz, 2 H), 5.32 (br s, 1 H), 4.62–4.55 (m, 2 H), 4.39 (dd, *J* = 13.9, 3.5 Hz, 1 H), 4.27 (br d, *J* = 13.9 Hz, 1 H), 3.45 (m, 4 H), 3.13 (m, 4 H). Anal. (C₁₈H₁₈F₃N₅O₆) C, H, N.

3-(3-[4-(Trifluoromethoxy)phenoxy]pyrrolidine (**103**) (Scheme 4A). Diethyl azodicarboxylate (6.57 mL, 38.7 mmol) was added dropwise to a refluxing solution of *tert*-butyl (3R)-3-hydroxypyrrolidine-1-carboxylate (**100**) (4.84 g, 25.9 mmol), 4-(trifluoromethoxy)phenol (**101**) (3.34 mL, 25.8 mmol), and triphenylphosphine (10.2 g, 38.9 mmol) in anhydrous THF (100 mL), and the solution was refluxed under N₂ for 5 h. The cooled solution was concentrated to dryness directly onto silica gel and chromatographed on silica gel. Elution with 3% EtOAc/petroleum ether gave foreruns, and then further elution with 17% EtOAc/petroleum ether gave the crude ether **102** as a colorless oil, which was used directly in the next step. A solution of this crude **102** in 1:1 CH₂Cl₂/TFA (120 mL) was stirred at 20 °C for 4 h. After concentration to dryness, the residue was partitioned between 1 N NaOH solution and CH₂Cl₂. The organic portion was acidified with 4 N HCl in dioxane and concentrated to dryness. The residue was triturated with petroleum ether and then dissolved in CH₂Cl₂. The solution was washed with 1 N NaOH, dried (Na₂SO₄), and concentrated under reduced pressure, to give **103** (3.93 g, 62% overall) as a pale-yellow oil. ¹H NMR (CDCl₃) δ 7.13 (d, *J* = 8.9 Hz, 2 H), 6.84 (d, *J* = 8.9 Hz, 2 H), 4.82–4.77 (m, 1 H), 3.21–3.13 (m, 2 H), 3.03 (dd, *J* = 12.6, 4.8 Hz, 1 H), 2.95–2.89 (m, 1 H), 2.13–2.04 (m, 1 H), 1.99–1.91 (m, 1 H). APCI MS *m/z* 248 [M + H]⁺.

(6S)-2-Nitro-6,7-dihydro-5H-imidazo[2,1-*b*][1,3]oxazin-6-yl (3S)-3-[4-(trifluoromethoxy)phenoxy]pyrrolidine-1-carboxylate (**83**) (Scheme 4C). Reaction of alcohol **6** with triphosgene and Et₃N, followed by reaction of the crude chloroformate with **103**, using

procedure J (except that the product was eluted from the silica gel column using EtOAc), gave **83** (39%) as a pale-yellow foam: mp 81–84 °C. ¹H NMR [(CD₃)₂SO] δ (1:1 mixture of amide rotamers) 8.06, 8.02 (2 s, 1 H), 7.30–7.21 (2 d, *J* = 8.5 Hz, 2 H), 7.07–6.97 (2 d, *J* = 8.5 Hz, 2 H), 5.27 (br s, 1 H), 5.01 (br s, 1 H), 4.60–4.52 (m, 2 H), 4.41–4.32 (m, 1 H), 4.28–4.21 (m, 1 H), 3.62–3.25 (m, 4 H), 2.18–1.99 (m, 2 H). HRFABMS calcd for C₁₈H₁₈F₃N₄O₇ *m/z* [M + H]⁺ 459.1128, found 459.1124. HPLC purity: 96.9%.

tert-Butyl 4-[[6-(trifluoromethyl)pyridin-3-yl]oxy]piperidine-1-carboxylate (106) (Scheme 4A). Diethyl azodicarboxylate (7.16 mL, 45.5 mmol) was added dropwise to a refluxing solution of *tert*-butyl 4-hydroxypiperidine-1-carboxylate (**104**) (6.10 g, 30.3 mmol), 6-(trifluoromethyl)pyridin-3-ol (**105**) (4.95 g, 30.3 mmol), and triphenylphosphine (11.9 g, 45.4 mmol) in anhydrous THF (80 mL), and the solution was refluxed for 5 h. The cooled solution was concentrated to dryness directly onto silica gel, and chromatographed on silica gel. Elution with 5% EtOAc/petroleum ether gave **106** (5.78 g, 55%) as a pale-yellow solid: mp 81–82 °C. ¹H NMR (CDCl₃) δ 8.37 (d, *J* = 2.7 Hz, 1 H), 7.61 (d, *J* = 8.7 Hz, 1 H), 7.29 (dd, *J* = 8.7, 2.7 Hz, 1 H), 4.61–4.57 (m, 1 H), 3.74–3.67 (m, 2 H), 3.41–3.34 (m, 2 H), 2.01–1.91 (m, 2 H), 1.83–1.73 (m, 2 H), 1.47 (s, 9 H). Anal. (C₁₆H₂₁F₃N₂O₃) C, H, N.

5-(Piperidin-4-yloxy)-2-(trifluoromethyl)pyridine (107). A solution of **106** (4.08 g, 11.8 mmol) in 1:1 CH₂Cl₂/TFA (50 mL) was stirred at 20 °C for 4 h. After concentration to dryness, the residue was partitioned between saturated aqueous NaHCO₃ solution and CH₂Cl₂. The aqueous portion was basified to pH = 14 with 1 N KOH, and the resulting mixture was extracted with CH₂Cl₂. Evaporation of this extract gave **107** (2.68 g, 92%) as a low melting solid that was used directly in the next step. ¹H NMR [(CD₃)₂SO] δ 8.42 (d, *J* = 2.8 Hz, 1 H), 7.79 (d, *J* = 8.7 Hz, 1 H), 7.63 (dd, *J* = 8.7, 2.8 Hz, 1 H), 4.66–4.59 (m, 1 H), 3.28 (br s, 1 H), 2.98–2.90 (m, 2 H), 2.62–2.55 (m, 2 H), 1.98–1.92 (m, 2 H), 1.52–1.42 (m, 2 H). HRFABMS calcd for C₁₁H₁₄F₃N₂O *m/z* [M + H]⁺ 247.1058, found 247.1059.

(6S)-2-Nitro-6,7-dihydro-5H-imidazo[2,1-b][1,3]oxazin-6-yl 4-[[6-(trifluoromethyl)pyridin-3-yl]oxy]piperidine-1-carboxylate (84) (Scheme 4C). Reaction of alcohol **6** with triphosgene and Et₃N, followed by reaction of the crude chloroformate with **107**, using procedure J (except that the product was eluted from the silica gel column using 5% MeOH/EtOAc), gave **84** (33%) as a cream solid: mp 105–106 °C. ¹H NMR [(CD₃)₂SO] δ 8.44 (d, *J* = 2.6 Hz, 1 H), 8.06 (s, 1 H), 7.82 (d, *J* = 8.7 Hz, 1 H), 7.65 (dd, *J* = 8.7, 2.6 Hz, 1 H), 5.31–5.26 (m, 1 H), 4.79 (m, 1 H), 4.60–4.54 (m, 2 H), 4.39 (dd, *J* = 13.9, 3.5 Hz, 1 H), 4.26 (d, *J* = 13.9 Hz, 1 H), 3.80–3.48 (br m, 2 H), 3.33–3.18 (br m, 2 H), 2.03–1.83 (br m, 2 H), 1.67–1.47 (br m, 2 H). Anal. (C₁₈H₁₈F₃N₅O₆) C, H, N.

N-Methyl-N-[4-(trifluoromethoxy)benzyl]piperidin-4-amine (112) (Scheme 4B). A solution of *tert*-butyl 4-aminopiperidine-1-carboxylate (**108**) (3.00 g, 15.0 mmol) and 4-(trifluoromethoxy)benzaldehyde (**109**) (2.14 mL, 15.0 mmol) in MeOH (60 mL) was refluxed for 4 h. After cooling to 20 °C, NaBH₄ (1.13 g, 29.9 mmol) was added in portions and the mixture was stirred for a further 30 min. Water was added, the mixture was extracted with EtOAc, and the extract was evaporated to give the crude amine **110** (5.75 g), which was used directly in the next step. A mixture of this crude **110** (5.75 g, 15.0 mmol), MeI (0.95 mL, 15.3 mmol), and K₂CO₃ (4.56 g, 33.0 mmol) in anhydrous acetone (150 mL) was stirred at 20 °C for 18 h. After removal of the solvent under reduced pressure, the residue was partitioned between CH₂Cl₂ and water, and the organic layer was evaporated to give *tert*-butyl 4-{methyl[4-(trifluoromethoxy)benzyl]-amino}piperidine-1-carboxylate (**111**) (4.77 g, 82% overall) as a crude solid: mp 35–40 °C, which was used directly in the next step. A solution of crude **111** (4.77 g, 12.3 mmol) in 1:1 CH₂Cl₂/TFA (150 mL) was stirred at 20 °C for 1 h. After concentration to dryness under reduced pressure, the residue was partitioned between 2 N NaOH and CH₂Cl₂, and the organic layer was evaporated to give **112** (3.16 g, 73% overall) as an oil. ¹H NMR (CDCl₃) δ 7.34 (d, *J* = 8.5 Hz, 2 H), 7.14 (d, *J* = 8.5 Hz, 2 H), 3.57 (s, 2 H), 3.22–3.16 (m, 2 H), 2.66–2.49 (m, 3 H), 2.19 (s, 3 H), 2.13 (br m, 1 H), 1.87–1.80 (m, 2 H), 1.59–1.48 (m, 2 H). HREIMS calcd for C₁₄H₁₉F₃N₂O *m/z* (M⁺) 288.1449, found 288.1448.

(6S)-2-Nitro-6,7-dihydro-5H-imidazo[2,1-b][1,3]oxazin-6-yl 4-[[methyl[4-(trifluoromethoxy)benzyl]amino]piperidine-1-carboxylate (85) (Scheme 4C). Reaction of alcohol **6** with triphosgene and Et₃N, followed by reaction of the crude chloroformate with **112**, using procedure J (except that the product was eluted from the silica gel column using 5% MeOH/EtOAc), gave **85** (39%) as a light-yellow solid: mp (Et₂O/petroleum ether) 55–58 °C. ¹H NMR [(CD₃)₂SO] δ 8.06 (s, 1 H), 7.40 (d, *J* = 8.5 Hz, 2 H), 7.27 (d, *J* = 8.5 Hz, 2 H), 5.26 (br s, 1 H), 4.60–4.51 (m, 2 H), 4.36 (dd, *J* = 13.8, 3.5 Hz, 1 H), 4.24 (br d, *J* = 13.8 Hz, 1 H), 4.01 (br m, 1 H), 3.79 (br m, 1 H), 3.53 (s, 2 H), 2.76 (br t, *J* = 12.4 Hz, 2 H), 2.60–2.51 (m, 1 H), 2.06 (s, 3 H), 1.79–1.63 (m, 2 H), 1.44–1.31 (m, 2 H). HREIMS calcd for C₂₁H₂₄F₃N₅O₆ *m/z* (M⁺) 499.1679, found 499.1677. HPLC purity: 97.3%.

Minimum Inhibitory Concentration Assays (MABA and LORA). These were carried out according to the published protocols.^{28,30}

Partition Coefficients. The octanol–water partition coefficients were measured using the shake-flask method, according to a published protocol.⁴¹

Solubility Determinations. *Method A.* Kinetic solubility assessments were made on powdered solids using a published protocol.¹⁶

Method B. The thermodynamic solubility of compound **82** (at pH = 1 and 7.4) was assessed by Cerep, 15318 NE 95th Street, Redmond, WA 98052, according to a published protocol (method C).¹⁵

Plasma Protein Binding Assay. The study of compound **82** was conducted by Cerep, 15318 NE 95th Street, Redmond, WA 98052, using an equilibrium dialysis technique with overnight incubation of the compound (at 10 μM, containing 1% DMSO), according to a published protocol.⁴²

hERG Assay. The study of the effect of compound **82** on cloned hERG potassium channels expressed in human embryonic kidney cells (HEK293) was conducted by ChanTest Corporation, 14656 Neo Parkway, Cleveland, OH 44128 (FASTPatch IC₅₀ screen).

Ames Test. Compound **82** (at concentrations of 0.25–250 μg/well) was evaluated in the microAmes reverse mutation screen conducted by Midwest BioResearch, LLC, 8025 Lamon Avenue, Skokie, IL 60077, testing against *Salmonella* strains TA98 and TA100 (preincubated both with and without rat liver S9).

Microsomal Stability Assays. These were conducted by MDS Pharma Services, 22011 30th Drive SE, Bothell, WA 98021–4444, using a published protocol.¹³ The percentage of compound remaining after a 1 h incubation was calculated as:

$$\% \text{ remaining} = 100 \times (\text{mean PAR}_{T60} / \text{mean PAR}_{T0})$$

where PAR = analyte/IS peak area ratio

In Vivo Acute TB Infection Assay. Each compound was administered orally to a group of 7 *M. tb*-infected BALB/c mice at a standard dose of 100 mg/kg, daily for 5 days a week for 3 weeks, beginning on day 11 postinfection, in accordance with published protocols.^{13,30} The results are recorded as the ratio of the average reduction in colony forming units (CFUs) in the compound-treated mice/the average CFU reduction in the mice treated with 1. In this assay, **1** caused up to 2.5–3 log reductions in CFUs.

In Vivo Chronic TB Infection 3 Week Assay. Compounds were administered orally as described for the acute assay but with treatment beginning ~70 days postinfection. In this assay, **1** caused a ca. 2 log reduction in CFUs, whereas **2** caused a ca. 3 log reduction in CFUs.

In Vivo Chronic TB Infection 8 Week Assay. Each compound was administered orally to a group of 7 *M. tb*-infected BALB/c mice at a dose of 30 mg/kg, daily for 5 days a week for 8 weeks, with treatment beginning ~50 days post infection. In this assay, **2** caused a ca. 3 log reduction in CFUs.

In Vivo Mouse Pharmacokinetics. Compounds were administered orally to CD-1 mice at a standard dose of 40 mg/kg, as a suspension in 0.5% carboxymethylcellulose/0.08% Tween 80 in water. Samples derived from plasma and lungs were analyzed by LC-MS/MS to generate the required pharmacokinetic parameters.

Studies of compounds **3**, **33**, and **82** were conducted at Cumbre Pharmaceuticals Inc., Dallas, Texas, and UNT Health Science Center,

3500 Camp Bowie Blvd., Fort Worth TX 76107–2699. The study of compounds **59** and **74** (using the same protocol) was conducted by MDS Pharma Services, 22002 26th Avenue SE, Suite 104, Bothell, WA 98021–4444.

In Vivo Rat Pharmacokinetics and Oral Bioavailability.

Compound **82** was administered to groups of 3 male Sprague–Dawley rats, both intravenously, at a single dose of 1 mg/kg, and orally, at a single dose of 20 mg/kg, as 1 or 2 mg/mL solutions in 40% hydroxypropyl- β -cyclodextrin/50 mM citrate buffer (pH = 3). Samples derived from plasma were analyzed by LC-MS/MS to generate the required pharmacokinetic parameters.

The study was conducted by Absorption Systems, 436 Creamery Way, Suite 600, Exton, PA 19341–2556.

In Vivo Dog Pharmacokinetics and Oral Bioavailability.

Compound **82** was administered to male beagle dogs (30 min post feeding), both intravenously (6 dogs), at a single dose of 2 mg/kg, and orally (3 dogs per group), at a single dose of 20 mg/kg, as 1 or 2 mg/mL solutions in 40% hydroxypropyl- β -cyclodextrin/50 mM citrate buffer (pH = 3). Oral dose groups were fed either a standard canine diet or a high fat FDA meal. Samples derived from plasma were analyzed by LC-MS/MS and the pharmacokinetic parameters were determined using Phoenix WinNonlin version 6.2 (Pharsight, CA, USA).

The study was conducted by ABC Laboratories, Inc., 4870 Discovery Drive, Columbia, MO 65201.

■ ASSOCIATED CONTENT

Supporting Information

Additional experimental procedures and characterizations for compounds; graphs of selected tabular data; combustion analytical data. This material is available free of charge via the Internet at <http://pubs.acs.org>.

■ AUTHOR INFORMATION

Corresponding Author

*Phone: (+649) 923 6145. Fax: (+649) 373 7502. E-mail: am.thompson@auckland.ac.nz.

■ ACKNOWLEDGMENTS

We thank the Global Alliance for Tuberculosis Drug Development for financial support through a collaborative research agreement. Special thanks belong to Drs. Anna Upton, Annette Shadiack, and Khisi Mdluli for their efforts in designing and coordinating the ADME/pharmacokinetic studies. The authors also thank Sisira Kumara and H. D. Sarath Liyanage, respectively, for the solubility and log *P* measurements, and Dr Kevin Hicks for his assistance with processing some pharmacokinetic data.

■ ABBREVIATIONS USED

TB, tuberculosis; MDR, multidrug-resistant; XDR, extensively drug resistant; *M. tb*, *Mycobacterium tuberculosis*; MIC, minimum inhibitory concentration; HIV, human immunodeficiency virus; CYP, cytochrome P450; SAR, structure–activity relationship; NMM, *N*-methylmorpholine; SD, standard deviation; DMSO, dimethyl sulfoxide; HLM, human liver microsomes; MLM, mouse liver microsomes; CFU, colony forming unit; HREIMS, high resolution electron impact mass spectrometry; HRFABMS, high resolution fast atom bombardment mass spectrometry; HRESIMS, high resolution electrospray ionization mass spectrometry; DMF, *N,N*-dimethylformamide; DIPEA, diisopropylethylamine; THF, tetrahydrofuran; TFA, trifluoroacetic acid; PAR, peak area ratio; IS, internal standard; AUC, area under the curve; DEAD, diethyl azodicarboxylate

■ REFERENCES

- (1) Koul, A.; Arnoult, E.; Lounis, N.; Guillemont, J.; Andries, K. The challenge of new drug discovery for tuberculosis. *Nature* **2011**, *469*, 483–490.
- (2) World Health Organization. *Global Tuberculosis Control: WHO Report 2010*. WHO Press: Geneva, Switzerland, 2010.
- (3) Laurenzi, M.; Ginsberg, A.; Spigelman, M. Challenges associated with current and future TB treatment. *Infect. Dis. Drug Targets* **2007**, *7*, 105–119.
- (4) Yew, W. W.; Cynamon, M.; Zhang, Y. Emerging drugs for the treatment of tuberculosis. *Expert Opin. Emerging Drugs* **2011**, *16*, 1–21.
- (5) Ginsberg, A. M. Drugs in development for tuberculosis. *Drugs* **2010**, *70*, 2201–2214.
- (6) Stover, C. K.; Warren, P.; VanDevanter, D. R.; Sherman, D. R.; Arain, T. M.; Langhorne, M. H.; Anderson, S. W.; Towell, J. A.; Yuan, Y.; McMurray, D. N.; Kreiswirth, B. N.; Barry, C. E.; Baker, W. R. A small-molecule nitroimidazopyran drug candidate for the treatment of tuberculosis. *Nature* **2000**, *405*, 962–966.
- (7) Matsumoto, M.; Hashizume, H.; Tomishige, T.; Kawasaki, M.; Tsubouchi, H.; Sasaki, H.; Shimokawa, Y.; Komatsu, M. OPC-67683, a nitro-dihydro-imidazoaxazole derivative with promising action against tuberculosis in vitro and in mice. *PLoS Med.* **2006**, *3*, 2131–2143.
- (8) Singh, R.; Manjunatha, U.; Boshoff, H. I. M.; Ha, Y. H.; Niyomrattanakit, P.; Ledwidge, R.; Dowd, C. S.; Lee, I. Y.; Kim, P.; Zhang, L.; Kang, S.; Keller, T. H.; Jiricek, J.; Barry, C. E. PA-824 kills nonreplicating *Mycobacterium tuberculosis* by intracellular NO release. *Science* **2008**, *322*, 1392–1395.
- (9) Manjunatha, U.; Boshoff, H. I. M.; Barry, C. E. The mechanism of action of PA-824: novel insights from transcriptional profiling. *Commun. Integr. Biol.* **2009**, *2*, 215–218.
- (10) Diacon, A. H.; Dawson, R.; Hanekom, M.; Narunsky, K.; Maritz, S. J.; Venter, A.; Donald, P. R.; van Niekerk, C.; Whitney, K.; Rouse, D. J.; Laurenzi, M. W.; Ginsberg, A. M.; Spigelman, M. K. Early bactericidal activity and pharmacokinetics of PA-824 in smear-positive tuberculosis patients. *Antimicrob. Agents Chemother.* **2010**, *54*, 3402–3407.
- (11) Ahmad, Z.; Peloquin, C. A.; Singh, R. P.; Derendorf, H.; Tyagi, S.; Ginsberg, A.; Grosset, J. H.; Nuernberger, E. L. PA-824 exhibits time-dependent activity in a murine model of tuberculosis. *Antimicrob. Agents Chemother.* **2011**, *55*, 239–245.
- (12) Dover, L. G.; Coxon, G. D. Current status and research strategies in tuberculosis drug development. *J. Med. Chem.* **2011**, *54*, 6157–6165.
- (13) Palmer, B. D.; Thompson, A. M.; Sutherland, H. S.; Blaser, A.; Kmentova, I.; Franzblau, S. G.; Wan, B.; Wang, Y.; Ma, Z.; Denny, W. A. Synthesis and structure–activity studies of biphenyl analogues of the tuberculosis drug (6*S*)-2-nitro-6-[[4-(trifluoromethoxy)benzyl]oxy]-6,7-dihydro-5*H*-imidazo[2,1-*b*][1,3]oxazine (PA-824). *J. Med. Chem.* **2010**, *53*, 282–294.
- (14) Sutherland, H. S.; Blaser, A.; Kmentova, I.; Franzblau, S. G.; Wan, B.; Wang, Y.; Ma, Z.; Palmer, B. D.; Denny, W. A. Synthesis and structure–activity relationships of antitubercular 2-nitroimidazoaxazines bearing heterocyclic side chains. *J. Med. Chem.* **2010**, *53*, 855–866.
- (15) Kmentova, I.; Sutherland, H. S.; Palmer, B. D.; Blaser, A.; Franzblau, S. G.; Wan, B.; Wang, Y.; Ma, Z.; Denny, W. A.; Thompson, A. M. Synthesis and structure–activity relationships of aza- and diazabiphenyl analogues of the antitubercular drug (6*S*)-2-nitro-6-[[4-(trifluoromethoxy)benzyl]oxy]-6,7-dihydro-5*H*-imidazo[2,1-*b*][1,3]-oxazine (PA-824). *J. Med. Chem.* **2010**, *53*, 8421–8439.
- (16) Thompson, A. M.; Sutherland, H. S.; Palmer, B. D.; Kmentova, I.; Blaser, A.; Franzblau, S. G.; Wan, B.; Wang, Y.; Ma, Z.; Denny, W. A. Synthesis and structure–activity relationships of varied ether linker analogues of the antitubercular drug (6*S*)-2-nitro-6-[[4-(trifluoromethoxy)benzyl]oxy]-6,7-dihydro-5*H*-imidazo[2,1-*b*][1,3]-oxazine (PA-824). *J. Med. Chem.* **2011**, *54*, 6563–6585.
- (17) Matsumoto, M.; Hashizume, H.; Tsubouchi, H.; Sasaki, H.; Itotani, M.; Kuroda, H.; Tomishige, T.; Kawasaki, M.; Komatsu, M.

Screening for novel antituberculosis agents that are effective against multidrug resistant tuberculosis. *Curr. Top. Med. Chem.* **2007**, *7*, 499–507.

(18) Ginsberg, A. M.; Laurenzi, M. W.; Rouse, D. J.; Whitney, K. D.; Spigelman, M. K. Safety, tolerability, and pharmacokinetics of PA-824 in healthy subjects. *Antimicrob. Agents Chemother.* **2009**, *53*, 3720–3725.

(19) Swain, C. J.; Williams, B. J.; Baker, R.; Cascieri, M. A.; Chicchi, G.; Forrest, M.; Herbert, R.; Keown, L.; Ladduwahetty, T.; Luell, S.; MacIntyre, D. E.; Metzger, J.; Morton, S.; Owens, A. P.; Sadowski, S.; Watt, A. P. 3-Benzyloxy-2-phenylpiperidine NK₁ antagonists: the influence of alpha methyl substitution. *Bioorg. Med. Chem. Lett.* **1997**, *7*, 2959–2962.

(20) Baker W. R.; Shaopei, C.; Keeler, E. L. Nitro-[2,1-*b*]imidazopyran compounds and antibacterial uses thereof. U.S. Patent 6,087,358, 2000.

(21) Kim, P.; Kang, S.; Boshoff, H. I.; Jiricek, J.; Collins, M.; Singh, R.; Manjunatha, U. H.; Niyomrattanakit, P.; Zhang, L.; Goodwin, M.; Dick, T.; Keller, T. H.; Dowd, C. S.; Barry, C. E. Structure–activity relationships of antitubercular nitroimidazoles. 2. Determinants of aerobic activity and quantitative structure–activity relationships. *J. Med. Chem.* **2009**, *52*, 1329–1344.

(22) Jiricek, J.; Patel, S.; Keller, T. H.; Barry, C. E.; Dowd, C. S. Preparation of nitroimidazole compounds useful in the treatment of infections caused by *Mycobacterium tuberculosis*, *Trypanosoma cruzi* or *Leishmania donovani*. Patent WO 2007075872 A2, 2007.

(23) Fletcher, S. R.; Hollingworth, G. J.; Jones, A. B.; Moyes, C. R.; Rogers, L. Preparation of heteroaromatic ureas which modulate the function of the vanilloid-1 receptor (VR1). Patent WO 2005028445 A2, 2005.

(24) Eckert, H.; Forster, B. Triphosgene, a crystalline phosgene substitute. *Angew. Chem., Int. Ed. Engl.* **1987**, *26*, 894–895.

(25) Wang, Q.; Huang, R. Synthesis and biological activity of novel *N'*-*tert*-butyl-*N'*-substituted benzoyl-*N*-(substituted phenyl)-aminocarbonylhydrazines and their derivatives. *Tetrahedron Lett.* **2001**, *42*, 8881–8883.

(26) Alberati-Giani, D.; Jolidon, S.; Narquizian, R.; Nettekoven, M. H.; Norcross, R. D.; Pinar, E.; Stalder, H. Preparation of 1-(2-aminobenzoyl)-piperazine derivatives as glycine transporter 1 (GlyT-1) inhibitors for treating psychoses. Patent WO 2005023260 A1, 2005.

(27) Collins, L. A.; Franzblau, S. G. Microplate Alamar blue assay versus BACTEC 460 system for high-throughput screening of compounds against *Mycobacterium tuberculosis* and *Mycobacterium avium*. *Antimicrob. Agents Chemother.* **1997**, *41*, 1004–1009.

(28) Cho, S. H.; Warit, S.; Wan, B.; Hwang, C. H.; Pauli, G. F.; Franzblau, S. G. Low-oxygen-recovery assay for high-throughput screening of compounds against nonreplicating *Mycobacterium tuberculosis*. *Antimicrob. Agents Chemother.* **2007**, *51*, 1380–1385.

(29) Lenaerts, A. J.; DeGroot, M. A.; Orme, I. M. Preclinical testing of new drugs for tuberculosis: current challenges. *Trends Microbiol.* **2008**, *16*, 48–54.

(30) Falzari, K.; Zhu, Z.; Pan, D.; Liu, H.; Hongmanee, P.; Franzblau, S. G. In vitro and in vivo activities of macrolide derivatives against *Mycobacterium tuberculosis*. *Antimicrob. Agents Chemother.* **2005**, *49*, 1447–1454.

(31) Brown, A.; Brown, T. B.; Calabrese, A.; Ellis, D.; Puhalo, N.; Ralph, M.; Watson, L. Triazole oxytocin antagonists: Identification of an aryloxyazetidone replacement for a biaryl substituent. *Bioorg. Med. Chem. Lett.* **2010**, *20*, 516–520.

(32) Boja, P.; Won, S.-W.; Suh, D. H.; Chu, J.; Park, W. K.; Lim, H.-J. Synthesis and biological activities of (4-arylpiperazinyl)piperidines as nonpeptide BACE 1 inhibitors. *Bull. Korean Chem. Soc.* **2011**, *32*, 1249–1252.

(33) Zheng, X.; Hodgetts, K. J.; Briemann, H.; Hutchison, A.; Burkamp, F.; Jones, A. B.; Blurton, P.; Clarkson, R.; Chandrasekhar, J.; Bakthavatchalam, R.; De Lombaert, S.; Crandall, M.; Cortright, D.; Blum, C. A. From arylureas to biaryl amides to aminoquinazolines: discovery of a novel, potent TRPV1 antagonist. *Bioorg. Med. Chem. Lett.* **2006**, *16*, 5217–5221.

(34) Zent, C.; Smith, P. Study of the effect of concomitant food on the bioavailability of rifampicin, isoniazid and pyrazinamide. *Tuberculosis Lung Dis.* **1995**, *76*, 109–113.

(35) Singh, B. N. Effects of food on clinical pharmacokinetics. *Clin. Pharmacokinet.* **1999**, *37*, 213–255.

(36) Hann, M. M. Molecular obesity, potency and other addictions in drug discovery. *Med. Chem. Commun.* **2011**, *2*, 349–355.

(37) Ryckmans, T.; Edwards, M. P.; Horne, V. A.; Correia, A. M.; Owen, D. R.; Thompson, L. R.; Tran, I.; Tutt, M. F.; Young, T. Rapid assessment of a novel series of selective CB₂ agonists using parallel synthesis protocols: a lipophilic efficiency (LipE) analysis. *Bioorg. Med. Chem. Lett.* **2009**, *19*, 4406–4409.

(38) Barry, C. E.; Slayden, R. A.; Sampson, A. E.; Lee, R. E. Use of genomics and combinatorial chemistry in the development of new antimycobacterial drugs. *Biochem. Pharmacol.* **2000**, *59*, 221–231.

(39) Hu, Y.; Coates, A. R. M.; Mitchison, D. A. Comparison of the sterilising activities of the nitroimidazopyran PA-824 and moxifloxacin against persisting *Mycobacterium tuberculosis*. *Int. J. Tuberculosis Lung Dis.* **2008**, *12*, 69–73.

(40) Gleeson, M. P. Generation of a set of simple, interpretable ADMET rules of thumb. *J. Med. Chem.* **2008**, *51*, 817–834.

(41) Hay, M. P.; Hicks, K. O.; Pruijn, F. B.; Pchalek, K.; Siim, B. G.; Wilson, W. R.; Denny, W. A. Pharmacokinetic/pharmacodynamic model-guided identification of hypoxia-selective 1,2,4-benzotriazine 1,4-dioxides with antitumor activity: the role of extravascular transport. *J. Med. Chem.* **2007**, *50*, 6392–6404.

(42) Banker, M. J.; Clark, T. H.; Williams, J. A. Development and validation of a 96-well equilibrium dialysis apparatus for measuring plasma protein binding. *J. Pharm. Sci.* **2003**, *92*, 967–974.

■ NOTE ADDED AFTER ASAP PUBLICATION

After this paper was published online December 29, 2011, a correction was made to the last paragraph before the Conclusions section. The revised version was published January 4, 2012.